JA

The Accretion Disk Limit Cycle Instability in Black Hole X-ray Binaries

J.K. Cannizzo, W. Chen, and M. Livio

SW9550

LABORATORY FOR HIGH ENERGY ASTROPHYSICS

National Aeronautics And Space Administration
Goddard Space Flight Center
Greenbelt, Maryland 20771

X-RAY: 95-22

THE ACCRETION DISK LIMIT CYCLE INSTABILITY IN BLACK HOLE X-RAY BINARIES

J.K. Cannizzo[1], W. Chen[1], and M. Livio[2],

Code 666
X-ray Astrophysics Branch
Laboratory for High Energy Astrophysics
NASA/Goddard Space Flight Center
Greenbelt, Maryland 20771

To appear in The Astrophysical Journal, Volume 454 (Dec 1, 1995)

[1]Universities Space Research Association and Code 661, NASA/GSFC
[2]Space Telescope Science Institute

ABSTRACT

We investigate the operation of the limit cycle mechanism in accretion disks around $\sim 10 M_\odot$ black holes. We explore a regime of parameter space relevant to these systems, and delineate a range of possible behaviors by testing the response of our one dimensional, time dependent, hydrodynamic model to variations in each of the control parameters in the theory. These parameters are: the number of radial grid points N, the accretor mass M_1, the inner disk radius $r_{\rm inner}$, the outer disk radius $r_{\rm outer}$, the mass transfer rate into the outer disk from the secondary star $\dot{M}_T$, and the accretion disk viscosity parameter α – parametrized in separate computations both in terms of radius (including a step function between low and high states) and in terms of local aspect ratio h/r.

For the class of models in which α is taken to vary in a step function between the two stable branches of accretion, we find a tendency for the outbursts to exhibit faster-than-exponential decays, in contrast to the observations. This behavior cannot be substantially affected by taking α to vary with radius – $\alpha \propto r^\epsilon$ – as in previous works, nor is it affected by the numerical resolution. Models in which α is a function of the local aspect ratio h/r can produce robustly exponential decays as observed if $\alpha \propto (h/r)^n$, where $n = 1.5$. This critical value for n is independent of the primary mass, unlike the critical ϵ value in the r^ϵ scaling. Numerically, we find that the transition front width is equal to the geometric average of h and r. (It is this fact which leads to the critical value $n = 1.5$ for exponential decay.) Previous studies have lacked the numerical resolution to make this determination, and in fact the specific results presented in earlier papers were probably severely compromised by grid spacing limitations. Finally, for models in which the decay is produced by accretion

onto the central object rather than by the action of a cooling front, we require $n = -2$ for exponential decays.

1. Background

The study of accretion disks has proven to be vital for understanding many diverse phenomena in astrophysics – e.g., interacting binary stars, young stellar objects, and active galactic nuclei. In this work we examine the possible role of time dependent accretion disk behavior in the black hole X-ray novae (BHXN) – semi-detached binary systems in which the Roche lobe filling mass donor star is a low-mass dwarf or subgiant and the accreting star is a black hole. Not long after the limit cycle mechanism was discovered and put forth as a possible explanation for the dwarf nova outbursts (Meyer & Meyer-Hofmeister 1981, Bath & Pringle 1982), it became obvious that such a mechanism might also apply to low mass X-ray binaries (Cannizzo, Wheeler, & Ghosh 1982, 1985).

The most well established BHXN are A0620-00 (Nova Mon 1975, orbital period $P_{\rm orb} = 7.75$ hr, mass function $f = 3.1 M_\odot$, McClintock & Remillard 1986), GS1124-68 (Nova Muscae, $P_{\rm orb} = 10.4$ hr, $f = 3.1 M_\odot$, Remillard, McClintock, & Remillard 1992), GS2023+338 (V404 Cyg, $P_{\rm orb} = 6.5$ days, $f = 6.3 M_\odot$, Casares, Charles, & Naylor 1992), GRO J1655-41 ($P_{\rm orb} = 2.6$ days, $f = 3.4 M_\odot$; Bailyn et al. 1995), H1705-250 (Nova Ophiuchi 1977, $P_{\rm orb} = 12.5$ hr, $f = 4.0 M_\odot$; Martin et al. 1995), and GS2000+25 ($P_{\rm orb} = 8.3$ hr, $f = 4.2 M_\odot$; Charles & Casares 1995). These systems were all discovered because of their X-ray outbursts, and subsequent optical identifications led to the determination that they were in binary systems. The X-ray outbursts exhibited by these systems tend to be long (compared to dwarf nova outbursts). Most have only lower limits on the recurrence times, since only one outburst has been observed. For A0620-00, outbursts occurred in 1917 and 1975, and for V404 Cyg, outbursts occurred in 1938 and 1989. During many of the brightest outbursts – e.g., those of A0620-00, GS2000+25, GS1124-68, GS2023+338, and GRO J0422+32 – the X-ray flux rises to maximum within a few days, and subsequently decays with an $e-$folding time of between about 30 to 60 days (White, Kaluzienski, & Swank

1984, van Paradijs & Verbunt 1984, Mineshige, Yamasaki, & Ishizaka 1993, hereafter MYI; Ebisawa et al. 1994). In addition, during the decay one sees secondary maxima in which the X-ray light can temporarily increase by about a factor of two before resuming its decay (Chen, Livio, & Gehrels 1993).

Previous workers investigated the possibility that the outbursts of the black hole X-ray binaries are caused by a limit cycle mechanism operating in the accretion disk (e.g., Huang & Wheeler 1989, Mineshige & Wheeler 1989, Ichikawa, Mineshige, & Kato 1994). The earlier studies were primarily interested in reproducing some features of the observed light curves, but did not attempt a thorough investigation with the aim of understanding uncertainties or shortcomings in the basic model. In the current work we perform a systematic parameter study of the limit cycle instability in an attempt to understand what realistic constraints can be placed on the model. More generally, we examine the question of what basic model is capable of explaining the fundamental observational characteristics of the outbursts seen in the BHXN.

2. Physical Considerations

The limit cycle mechanism has been well established and tested as a model for outbursts in dwarf novae, and a detailed comparison between theory and observation has been carried out. In part this was possible because of the existence of an extremely large data base (e.g., Cannizzo 1993b, hereafter C93b). The observations of the BHXN are not nearly as complete: in most instances our knowledge of the outburst properties of these systems are based on a single outburst. Nevertheless, by assuming the limit cycle mechanism to be at work in these systems, there are certain inferences we can draw based on the existing observations.

One of the fundamental principles concerning the limit cycle is that, at a given annulus

in the disk, there is a range of local mass transfer rates within which the instability can operate. This range spans the regime from $\dot{M}_{\rm max} = \dot{M}(\Sigma_{\rm max})$ to $\dot{M}_{\rm min} = \dot{M}(\Sigma_{\rm min})$, which encompasses a dynamic range of about a factor of 10 (Cannizzo, Shafter, & Wheeler 1988, hereafter CSW). Given that the local maxima and minima in $\Sigma(T_{\rm eff})$ lie at roughly the same $T_{\rm eff}$ independent of radius, the critical accretion rates associated with these extrema vary roughly as r^3. This comes about because of the local condition $\sigma T_{\rm eff}^4 = (3/8\pi)GM\dot{M}r^{-3}$ (Shakura & Sunyaev 1973) through which $T_{\rm eff}$ depends on the function $\dot{M}r^{-3}$. The disk spans a rather wide range in radius, so the actual unstable range, given by $\gamma = \dot{M}_{\rm min}(r_{\rm outer})/\dot{M}_{\rm max}(r_{\rm inner})$ is large. Another way of stating this is that the disk will be globally unstable if the rate of mass transfer from the secondary star into the outer accretion disk is less than $\dot{M}_{\rm min}(r_{\rm outer})$ and greater than $\dot{M}_{\rm max}(r_{\rm inner})$. For a typical dwarf nova above the period gap, $r_{\rm outer}/r_{\rm inner} \sim 100$, so $\gamma \sim 10^7$. For a $\sim 10 M_\odot$ black hole (with the last stable orbit at $\sim 10^7$ cm) in a binary with $P_{\rm orbit} \sim 8$ hr, $\gamma \sim 10^{13}$. One consequence of this large dynamic range of unstable behavior is that, in quiescence, the maximum allowed rate of accretion onto the black hole is small – i.e., the rate of mass loss from the inner annulus onto the central object cannot exceed $\dot{M}_{\rm max}(r_{\rm inner})$ or else the instability would have already been triggered. Taking the expression for $\dot{M}_{\rm max}$ from CSW ($\dot{M}_{\rm max} = 10^{15}$ g s^{-1} $r_{10}^{2.6} m_1^{-0.87}$) and adopting $r_{\rm inner} = 10^7$ cm and $M_1 = 10 M_\odot$ gives $\dot{M}_{\rm max} \sim 10^6$ g s^{-1}. This low value contradicts observations (Lasota 1995). For example, McClintock, Horne, and Remillard (1995) infer a quiescent accretion rate onto the central object of about $10^{10} - 10^{11}$ g s^{-1} in A0620-00, and Wagner et al. (1994) infer a quiescent rate of about 10^{12} g s^{-1} in V404 Cyg. These rates are much smaller than the mass transfer rates between the two stars. Moreover, the characteristic temperatures derived from fitting a blackbody spectrum to the quiescent X-ray fluxes are orders of magnitude larger than in the model (e.g., ~ 0.2 keV for V404 Cyg from Wagner et al. 1994 versus a few tenths of an eV for the model temperatures in quiescence).

It has long been known that this discrepancy between theory and observation exists for dwarf novae: the disk instability model works well to account for outbursts, but not for explaining the levels of UV and X-ray flux observed in quiescence. It is interesting that the margin of disagreement between theory and observation in terms of accretion rate onto the compact object during quiescence is also large for dwarf novae: taking $r_{\rm inner} \simeq R(\text{white dwarf}) \simeq 10^{8.7}$ cm and $M_1 \simeq 1 M_\odot$ gives $\dot{M}_{\rm max} \sim 10^{11.6}$ g s^{-1} for the upper limit allowed by theory, whereas the rates inferred from observations of dwarf novae are $\sim 10^{14} - 10^{15}$ g s^{-1} (Eracleous, Halpern, & Patterson 1991, Mukai & Shiokawa 1993). Thus the ratio of observed to theoretically allowed rates of accretion in quiescence is $\sim 10^3$.

Clearly, if the limit cycle instability is to apply to these systems, then some mechanism extrinsic to the limit cycle must cause the inner edge to drain in such a manner that the local evaporation is not communicated through the vertical disk structure as an increase in effective temperature. Such a mechanism could be produced by a disk wind, which in itself may be driven by coronal activity, if the disk viscosity is dynamo driven (Armitage, Livio, & Pringle 1995). In our modeling with $\alpha = \alpha_0 (h/r)^n$ (where h is the local disk semithickness and r is the local radius), where we try to reproduce the observed BHXN light curves, we might have considered the additional process of material extraction from the inner edge at a rate inferred from observations of A0620-00. This would have depleted the surface density in the inner edge by some fraction. Also, Meyer & Meyer-Hofmeister (1994) discuss a physical evaporation mechanism which may operate in quiescence in dwarf novae, to account for the quiescent flux seen in the EUV and X-ray. A similar mechanism may also work in quiescence in the black hole binaries to produce the observed fluxes (e.g., Narayan & Yi 1995).

There is another aspect of the problem which can be addressed in simple terms, without the need for computations. In their formulation of the theory of the recurrence

time for outbursts in the limit cycle model, CSW defined a dimensionless secondary mass transfer rate $\zeta \equiv \dot{M}_T/\dot{M}_{\rm min}(r_{\rm outer})$. For high mass transfer rates such that $\zeta > 1$, the entire disk is always ionized and resides permanently on the upper branch of solutions. For lower mass transfer rates such that $\zeta < 1$, the disk is prone to the limit cycle instability. One of the strengths of the model has been that the observed dividing point in mass transfer rate between those systems permanently stuck in a high state, and those exhibiting outbursts, agrees with the theoretical value corresponding to $\zeta = 1$ (Smak 1983). For most dwarf novae which have been well studied, $0.1 \lesssim \zeta \lesssim 1$, and the duty cycle for bursting behavior is also large, in fact comparable to ζ. Now, for the BHXN it appears that both quantities are much smaller. For instance, a simple estimate for the secondary mass transfer rate in A0620-00 by McClintock et al. (1983) using the total energy released in the 1975 outburst and the recurrence time of $\sim$ 58 yrs gives $\dot{M}_T \sim 2 \times 10^{15}$ g s^{-1}. Using the expression for $\dot{M}_{\rm min}$ from CSW ($\dot{M}_{\rm min} = 10^{16}$ g s^{-1} $r_{10}^{2.6} m_1^{-0.87}$), taking $M_1 = 10 M_\odot$ and $r_{\rm outer} = 1.4 \times 10^{11}$ cm gives $\sim 1.3 \times 10^{18}$ g s^{-1}, hence $\zeta \sim 10^{-3}$. In other words, the mass transfer rate would have to be about a thousand times higher in A0620-00 for the disk to be stable in the high state. Furthermore, the duty cycle for bursting behavior in A0620-00 is about 200 d/60 yr $\sim 10^{-2}$, again in line with the small ζ value. Recurrence times for the other bright systems like A0620-00 might plausibly be one to several decades.

We comment briefly on irradiation of the outer portions of the disk by X-ray flux produced near the inner edge. Tuchman, Mineshige, & Wheeler (1990) and Mineshige, Tuchman, & Wheeler (1990) have discussed the effect of irradiation on the vertical structure of the disk. There are two main issues regarding the irradiation:

(1) How important is reprocessing of X-ray flux into optical flux?

(2) Can irradiation affect the propagation of the cooling front?

It seems probable that most of the optical flux is indeed reprocessed X-ray flux,

and, furthermore, for low mass X-ray binaries in which orbital periods and mass transfer rates have been deduced, irradiation is capable of keeping the disk in the high state. A well-studied example is Sco X-1, a neutron star binary with $P_{\rm orbital} = 18.9$ hr (Gottlieb, Wright, & Liller 1975). The inferred binary mass transfer rate is $\sim 10^{-9} M_\odot$ yr^{-1} (Vrtilek et al. 1991), so that $\zeta \sim 0.01$, and yet the accretion disk appears to be in a permanent high state. (The flux varies by only about a factor of two.) If $\dot{M}(r)$ is constant, then the disk has a concave shape when seen in cross-section (Shakura & Sunyaev 1973), such that the surface of the disk at all radii is directly exposed to the strong source of X-ray flux from near the inner edge. For systems showing outbursts, however, the $\dot{M}(r)$ profile is not constant with r. As shown by Cannizzo (1994), the flow pattern within the disk leads to an overall disk shape which is convex rather than concave, when viewed in cross-section. This convex shape shields the outer part of the disk from direct irradiation. Therefore direct irradiation should not play a role in affecting systems with outbursts. It is not clear what the effect of indirect irradiation by a scattering might be.

3. Model

The accretion disk limit cycle model has been described in many recent review articles (e.g. Meyer-Hofmeister & Ritter 1990, Livio 1994, Cannizzo 1993a). The physical cause for the instability is a hysteresis relation between the local mass flow rate (or local effective temperature) and the disk surface density Σ. This hysteresis is sometimes referred to as the "S-curve". There are two allowed physical states within which an element of gas at a given radius in the disk can reside: a "low viscosity" state which constitutes the lower branch of the "S", and a "high viscosity" state which constitutes the upper branch of the "S". Associated with each annulus in the disk, there exists a critical surface density $\Sigma_{\rm max}$, above which the disk must be in a state of high viscosity, and another critical surface density $\Sigma_{\rm min}$,

below which the disk must be in a state of low viscosity. The turning point of the S-curve at the terminus of the upper branch defines $\Sigma_{\rm min}$, and the turning point of the S-curve at the terminus of the lower branch defines $\Sigma_{\rm max}$. The model operates as follows: Material accumulates in a quiescent stage, during which time, the viscous time scale for matter transport within the disk is very long compared to the mass transfer time scale for matter arriving from the mass losing star. Matter piles up in the disk until $\Sigma(r) > \Sigma_{\rm max}(r)$ at some radius r. The level of viscous dissipation then increases dramatically, and this increase is communicated to the adjacent portions of the still dormant disk through waves of enhanced surface density which propagate both to smaller and larger radii. These pulses boost the local surface density at each radius above $\Sigma_{\rm max}$, thereby eventually initiating heating at all radii. This heating drives most or all of the disk from the lower branch of the S-curve to the upper branch. After this stage has ended, the disk finds itself in a high viscosity stage wherein the viscous time is shorter, and material begins to flow onto the central object. As this occurs, the surface density in the outer regions of the disk drops, until, at some point, $\Sigma(r_{\rm outer})$ is less than $\Sigma_{\rm max}(r_{\rm outer})$. This begins a cooling wave which propagates inward and reduces the local surface density at each radius below $\Sigma_{\rm min}$, so that the disk reverts back to the low state. The outburst has ended and the quiescent interval begins again.

The general numerical model we employ is described in detail in C93b and Cannizzo (1994). One of the changes that we introduce in the present work is that we allow the viscosity parameter α to have the form $\alpha = \alpha_0(h/r)^n$. The usual finding from modeling dwarf nova outbursts has been that, in order to obtain well defined outbursts, α must be larger in outburst than in quiescence. This is achieved by using one value of α along the lower stable branch of solutions ($\alpha_{\rm cold}$) and another along the upper branch ($\alpha_{\rm hot}$), or through an $\alpha_0(h/r)^n$ prescription (Meyer & Meyer-Hofmeister 1983), or some more complicated procedure (Ichikawa & Osaki 1992). For any of these methods there are basically two free parameters which characterize α. One of the deficiencies in the class of

models in which α varies in a step function between the low and high states (but is constant with radius), is that the outbursts tend to start at the inner disk edge (Lin, Papaloizou, & Faulkner 1985, C93b, Ludwig et al. 1994). This tends to lead to outbursts with slow rise times. Although some dwarf novae have slow rise outbursts, many also have fast rise outbursts which are consistent with a triggering at large radii. For full generality, it is probably a strength of the model to be able to produce outbursts which can begin at any radius in the disk.

The time dependent model and steady state scalings we use are similar to those given in C93b. The S-shaped curve which gives the relation between the effective temperature and surface density was simplified to two straight lines (in log-log space). One change we have made is a generalization of the scaling for the low state. Eqn. (13) of C93b gives the scaling for $T_e(\mathrm{cold})(\Sigma, \alpha_{\mathrm{cold}}, r)$. In that expression, $a_1 \equiv d\log T_e(\mathrm{cold})/d\log\Sigma = 0.75$. This value was taken to be representative of values obtained through vertical structure calculations. In view of the uncertainties associated with those works, we do not fix a_1 to be 0.75 in the present work. Instead, it can be varied somewhat depending on the specific model. The general law is

$$T_{\mathrm{cold}} = B_2 \Sigma^{a_2} \alpha_{\mathrm{cold}}^{b_2} m_1^{c_2/3} r_{10}^{-c_2}, \tag{1}$$

where $B_2 = 7.89 \times 10^{-11} B_1^4$, $B_1 = 5870/17.677^{a_1}$, $a_2 = 4a_1 - 1$, $b_2 = 4b_1 - 1$, $c_2 = 4c_1 - 1.5$, $b_1 = 0.7a_1$, $c_1 = 1.1a_1 + 0.1$, $m_1 = M_1/1M_\odot$, and $r_{10} = r/10^{10}$ cm (Meyer & Meyer-Hofmeister 1981, Pringle, Verbunt, & Wade 1986). For models in which $\alpha = \alpha_0(h/r)^n$ we have

$$T_{\mathrm{cold}}^{1-b_2 n/2} = B_2 \, \Sigma^{a_2} \, \alpha_0^{b_2} \left(\frac{\sqrt{\mathcal{R}}}{\Omega r}\right)^{b_2 n} m_1^{c_2/3} \, r_{10}^{-c_2}, \tag{2}$$

where $\mathcal{R}$ is the ideal gas constant and Ω is the (Keplerian) angular velocity.

4. Parameter Study for Models in which $\alpha = f(r)$

We first discuss the results of a parameter study within the paradigm in which α is independent of radius and varies in a step function between the lower and upper branches of the S-curve. We adopt one value of $\alpha_{\rm cold}$ for the lower stable branch of solutions, and another value $\alpha_{\rm hot}$ for the upper branch. For our "standard" or default model in this section we take $\alpha_{\rm cold} = 0.01$, $\alpha_{\rm hot} = 0.1$, a mass transfer rate $\dot{M}_T = 6.3 \times 10^{16}$ g s^{-1}, primary mass $M_1 = 10 M_\odot$, and outer disk radius 1.5×10^{11} cm. For the slope of the lower branch of the S-curve we take $a_1 \equiv d \log T_{\rm eff}/d \log \Sigma = 5$. For the parameters used to study the BHXN, we find that the value $a_1 = 0.75$ used by C93b leads only to irregular fluctuations in the luminosity, but not to regular outbursts. A larger value of a_1 is required to lower the effective viscosity in the low state. We interpolate α logarithmically according to midplane temperature between the lower and upper branches, where the midplane temperature is that calculated at a given radius and time from solving the thermal energy equation. The outbursts which occur under the assumption of $\alpha_{\rm hot}/\alpha_{\rm cold} \simeq 10$ tend to be relatively flat topped, and this stage is followed by a rate of faster decay. The flat top is due to the same physics as discussed in C93b for the "long" outbursts in SS Cyg – namely, that large ratio of alphas leads to a large ratio of $\Sigma_{\rm max}/\Sigma_{\rm min}$, and after an outburst has been triggered, significant mass must drain from the inner edge onto the accretor before the surface density at the outer disk edge has dropped to the point that the cooling front can begin to propagate.

One of the limitations imposed on the class of models discussed in this section arises from the assumption that α is independent of radius. The thermal time scale $\sim 1/(\alpha\Omega)$ sets the time step used in the computations via the thermal energy equation. When a transition front exists at small radii near the black hole the requisite time step becomes extremely small. Because of this limitation we are not able to take an inner radius smaller than about

10^8 cm, and we are limited to no more than 200 grid points.

The parameters we investigate in this section are the inner disk radius $r_{\rm inner}$, the mass transfer rate from the secondary star into the outer edge of the accretion disk $\dot{M}_T$, the alpha parameter in the low state $\alpha_{\rm cold}$, the central object mass M_1, and the outer disk radius $r_{\rm outer}$. In the following tables we show seven quantities associated with the outbursts: (1) the recurrence time for outbursts, (2) the rise time for the light curve (obtained by calculating the rate of accretion at the inner edge) to change by a factor of 10^3 – measured from the peak of the outburst, (3) the rise time for the flux to vary by 10^2 – again measured from the time of $\dot{M}_{\rm peak}$, (4) the rise time for the flux to vary by e, (5) the decay time for the flux to drop by e – measured from the time of $\dot{M}_{\rm peak}$, (6) the amount of time spent on the plateau part of the outburst, and (7) the value of $\dot{M}_{\rm peak}$. It is important to note that, although the time scales given by (4) and (5) are cast in terms of e–folding times, the functional form characterizing the outburst shape does not have an exponential shape for models in which $\alpha = f(r)$: the plateau of the outburst has a slower-than-exponential form, and the decay after the plateau has a faster-than-exponential form. Thus the e–fold times in the tables are not to be confused with those of the next section.

Table 1 presents the results of a series of computations in which we vary $r_{\rm inner}$. This is achieved by keeping the grid point spacing fixed and changing the innermost range of the grid. In effect we are eliminating grid points from the inner regions of the disk by doing this. The time scales we calculate are computed from following the outbursts defined by the rate of mass loss from the inner disk. As we can see, the outburst properties are relatively unaffected by the value of $r_{\rm inner}$ for our "standard model". As $r_{\rm inner}$ is made to decrease, there is a very slight decrease in the recurrence time scale, and a somewhat larger increase in the time scales directly associated with the individual outbursts – i.e., the rise and decay times. The duration of the plateau stage of the outbursts is about 1 yr, and the

time to decay by a factor of e from the peak is $\sim$ 160 d. For these outbursts, the peak in the rate of accretion onto the black hole is 10^{19} g s^{-1}. Since the Eddington luminosity is $L_{\rm Edd} \sim 10^{38}$ erg s^{-1} $(M_1/M_\odot)$, and the accretion luminosity is $L_{\rm acc} \sim 0.1\dot{M}c^2$, the peak rate of accretion is of order of the Eddington critical rate.

Table 2 shows the dependence of outburst properties on $\dot{M}_T$. There is very nearly an inverse correlation between recurrence time for outbursts and $\dot{M}_T$. For our adopted a_1 value, the viscous dissipation in quiescence is small, and the disk mass stored by the time $\Sigma_{\rm max}$ is exceeded is close to the "maximum mass" $M_{\rm max} \equiv \int 2\pi r' dr' \Sigma_{\rm max}(r')$ (CSW). There is virtually no effect on the time scales associated with the individual outbursts as $\dot{M}_T$ varies. This is as one might naively expect, given that these time scales are dependent on viscous and thermal processes whose rates are determined mainly by α.

Table 3 shows the effect of varying $\alpha_{\rm cold}$ while keeping $\alpha_{\rm hot}$ constant. The recurrence times for outbursts varies inversely with $\alpha_{\rm cold}$ because $\alpha_{\rm cold}$ controls the critical surface density $\Sigma_{\rm max}$ which sets the amount of disk material in the quiescent state. The decreasing disk mass for larger $\alpha_{\rm cold}$ also causes a decrease in the amount of time spent on the viscous plateau, and the peak level of accretion.

Table 4 shows the effect of varying the primary mass M_1. As M_1 increases, there is a weak decrease in the recurrence time, consistent with the fact that $\Sigma_{\rm max} \propto M_1^{-0.35}$, and $t_{\rm recurrence} \propto \Sigma_{\rm max} r_{\rm outer}^2$. We also see a general increase in the time scales associated with outbursts – the rise and decay times. The reason for this is that the equilibrium disk mass becomes smaller as M_1 increases, thus at a given radius h/r also decreases, and the thermal and viscous times increase. The inverse correlation between the peak accretion rate and M_1 is also consistent with the decreasing equilibrium disk mass.

Table 5 shows the effect of varying $r_{\rm outer}$. The effective mass of the stored material varies as $r_{\rm outer}^3$. This comes about because $M_{\rm disk}(r) = \int^r 2\pi r' dr' \Sigma(r')$, and in quiescence

$\Sigma(r) \sim \Sigma_{\rm max}(r)$, where $\Sigma_{\rm max} \propto r$. Hence the recurrence time $t_{\rm rec}$ also varies as $r^3_{\rm outer}$ (CSW). The general response of the temperature of gas in a given annulus to an increase in the mass at that annulus (i.e., the surface density) is a concurrent increase. This increases the viscous dissipation and decreases the viscous and thermal time scales which accompany outbursts. It may therefore seems paradoxical in Table 5 that as the disk mass increases, the time scales associated with individual outbursts (i.e., the rise and decay times) also increase. The reason for this is that the disk mass is being made to lie at progressively larger radii, and the increasing time scales are due to the increasing amount of time required to move material from the outer disk to the inner disk.

Cannizzo (1994) studied the decay rate of the optical flux following the decline from maximum in dwarf novae outbursts and found that, for parameters relevant to dwarf novae, roughly exponential decays could be produced if $\alpha \propto r^{0.3} - r^{0.4}$. Consequently, we attempted such a radial dependence of the viscosity parameter here. Figure 1 shows the results of taking $\alpha \propto r^{\epsilon}$, where ϵ is varied in increments of 0.1 between 0 and 0.5. *All the runs shown seem to have a faster than exponential form, and a flat-topped plateau.* The difficulty in obtaining exponential decays with the $\alpha \propto r^{\epsilon}$ prescription leads us to believe that this functional form may not be the right one (i.e., the one nature has chosen). Although Cannizzo (1994) could get a marginally acceptable exponential decay of the light curve for dwarf nova parameters, the exponentiality was not very robust. For example, for a given ϵ, varying the central object mass affects the form of the decay. In light of this consideration, we will not consider the r^{ϵ} scaling further in this paper.

5. Parameter Study for Models in which $\alpha = g(h/r)$

5.1. Steady State Considerations

The results of the previous section and of Cannizzo (1994) reveal the inadequacies of models of the type $\alpha \propto r^{\epsilon}$ in producing decays which are robustly exponential. We now investigate the class of models for which $\alpha = \alpha_0 (h/r)^n$. This form has been used by many limit cycle disk instability modelers, beginning with Meyer & Meyer-Hofmeister (1984), and may have some physical basis (e.g., Meyer & Meyer-Hofmeister 1983; Vishniac & Diamond 1992). Recent work on the magnetorotational instability for viscous dissipation in accretion disks (Balbus & Hawley 1991) has not advanced to the stage where one can make any statement about the functional dependence of α (Hawley, Gammie, & Balbus 1995). The parametrizations used for the steady state $T_e(\Sigma)$ relations are the same as described earlier. In the previous section we utilized the physics of $\Sigma_{\rm max}$ associated with the convection effect (see C93b for a description). The midplane temperature associated with this local maximum in $\Sigma(T_{\rm eff})$ in the steady state solutions lies at $T \sim 15,000$ K. Various workers (e.g., Mineshige & Osaki 1983, Pojmański 1986, Cannizzo 1992, Ludwig et al. 1994) have shown how the value of $\Sigma_{\rm max}$(convective) depends on factors such as the ratio of mixing length to local pressure scale height in the disk which enter into the prescription for convection. These workers and others have investigated the vertical structure of accretion disks and shown that there are actually two separate hysteresis curves in the steady state $T_{\rm eff} - \Sigma$ relation – one due to the changing strength of convection as $\dot{M}$ is made to vary, and one based on the very steep temperature dependence of the opacity at $T \sim 6000 - 8000$ K (see also Faulkner et al. 1983). The midplane temperature associated with the convective effect maximum $\Sigma_{\rm max}$(convective) is about 15,000 - 20,000 K, and that associated with the opacity effect maximum $\Sigma_{\rm max}$(opacity) is about 6000-8000 K.

In the course of numerical experimentation using models with the local maximum determined from the convective effect, we find that, for the models in which $\alpha = \alpha_0(h/r)^n$, one cannot produce enough of a variation in the integrated viscous stress $W \equiv \int_{-h}^{+h} \alpha P(z')dz'$ in going from $\Sigma_{\rm min}$ to $\Sigma_{\rm max}$ to allow the creation and propagation of transition fronts in the disk. The reason for this is that the ratio of midplane temperatures between $\Sigma_{\rm min}$ and $\Sigma_{\rm max}$(convective) in the steady state solutions is only about 2 (Cannizzo & Wheeler 1984), and since the kinematic viscosity coefficient varies as $T_{\rm midplane}$, the jump in viscosity in going from the low to high state is small. The fact that we now also have $\alpha \propto (h/r)^n$ (where $h \propto \sqrt{T_{\rm midplane}}$) increases the jump slightly, but not enough to make a difference. (Smak 1984 first showed that there must be a rather large increase in the viscosity in going between the two states, or else the model is incapable of producing large and well-separated outbursts.) The narrow dynamic range in viscosity between $T_{\rm midplane}(\Sigma_{\rm min})$ and $T_{\rm midplane}(\Sigma_{\rm max}[{\rm convective}])$ cannot be made appreciably larger through judicious choices of α_0 and n. There was no similar problem in the amplitude of the jump in W between the low and high states for models of the type discussed in the previous section, because the step function character of the jump in α between the two states artificially ensures a large jump in W. We conclude, therefore, that if $\alpha = \alpha_0(h/r)^n$ is the correct scaling, then the relevant local maximum is that produced by the opacity effect, and not that produced by the convective effect. The ratio $T_{\rm midplane}(\Sigma_{\rm min})/T_{\rm midplane}(\Sigma_{\rm max}[{\rm opacity}]) \simeq 5$ is sufficient to ensure the production of large and well separated outbursts in the limit cycle model. To complicate matters further, it is conceivable that α could be a function which varies as $(h/r)^n$ within the hot branch, and then jumps discontinuously to a much smaller value in quiescence (Armitage et al. 1995). In that case the arguments used in this paragraph would not apply – that is, one could not exclude having $\Sigma_{\rm max}$(convective) trigger the instability.

Although the viscosity parameter α is now allowed to vary depending on local conditions, the values $\alpha(\Sigma_{\rm max})$ and $\alpha(\Sigma_{\rm min})$ are dependent only on radius. The values of

the midplane temperature at the turning points in the S-curve depend on α, which now depends on temperature through the h/r scaling. Solving the relevant expressions for T gives:

$$T_{\rm max}^{1+(n/2)(s_1a_2-b_2)} = 0.266^{s_1a_2} B_2\ S_1^{a_2}\ {\alpha_0}^{b_2-a_2s_1} \left(\frac{\sqrt{\mathcal{R}}}{\Omega r}\right)^{n(b_2-a_2s_1)} r_{10}^{1.1a_2-c_2}\ m_1^{-(1.1a_2-c_2)/3}, \quad (3)$$

where $T_{\rm max} = T_{\rm midplane}(\Sigma_{\rm max})$ – the temperature at the upper terminus of the lower branch, $S_1 = 10^{1.65}$, and $s_1 = 0.7$; and

$$T_{\rm min}^{1+(n/14)(3s_2-1)} = 9755\ (0.266^{s_2} S_2)^{3/7}\ \alpha_0^{(1-3s_2)/7} \left(\frac{\sqrt{\mathcal{R}}}{\Omega r}\right)^{(1-3s_2)n/7} r_{10}^{9/140}\ m_1^{-3/140}, \quad (4)$$

where $T_{\rm min} = T_{\rm midplane}(\Sigma_{\rm min})$ – the temperature at the lower terminus of the upper branch, $S_2 = 10^{1.35}$, and $s_2 = 0.7$.

5.2. Numerical Results

Figure 2 shows the results of a numerical experiment in which we simulate the decay of an outburst. This is accomplished by taking an initial surface density profile $\Sigma(r) \propto r^{-3/4}$ characteristic of the standard Shakura & Sunyaev (1973) steady state disk, and putting all grid points in the high temperature state. This would correspond to conditions in the disk near the time of maximum light in an outburst after the heating front had just finished transforming the entire disk to the upper stable branch of the S-curve. For our initial profile $\Sigma(r_{\rm outer}) = 0.95\Sigma_{\rm min}(r_{\rm outer})$ and $T(r) = T_{\rm hot}(r)$ for all r. This initial condition ensures the immediate creation of a cooling front at the outer edge. For these runs we take $r_{\rm inner} = 10^7$ cm, $r_{\rm outer} = 1.5 \times 10^{11}$ cm, and $M_1 = 10 M_\odot$. Figure 2 shows the evolution of Σ, T, and α during the decay of an outburst. The pattern is much the same as that found in previous

works. The dashed lines in each panel show conditions at $\Sigma_{\rm max}$ and $\Sigma_{\rm min}$. The calculated radial profiles of Σ and T within the hot part of the disk follow roughly the standard $r^{-3/4}$ Shakura & Sunyaev (1973) law. The viscosity parameter α increases very weakly with radius out to the hot/cold interface, and then falls markedly going into the cold region.

5.2.1. Effect of Varying Number of Grid Points

Figure 3 shows the results of experiments in which the number of grid points in the radial direction N is varied between 300 and 1000. The motivation for going through this exercise is the finding by C93b of the effect on the computed light curves caused by varying N. It is import to take enough grid points so that the small scale features in the transition fronts are well resolved. For our adopted parameters, $r_{\rm outer}/r_{\rm inner} \simeq 10^4$, we cannot cover the dynamic range in disk radii with our grid spacing using less than about 300 points. The first panel shows the "light curves" determined from the rate of accretion at the inner disk edge. (We are implicitly assuming that the observed soft plus hard X-ray fluxes from BHXN correspond directly to the rate of accretion onto the central object.) The second panel contains curves showing the locally defined $e-$folding decay time $t_{\rm e-fold} \equiv |d \ln \dot{M}_{\rm inner}/dt|^{-1}$ corresponding to each light curve in the first panel. Note that, for smaller N, we systematically overestimate $t_{\rm e-fold}$. The reason for this can be understood at least partially by considering the third panel. This shows the number of grid points contained within the cooling front N_F, as a function of radius. In the code, we define an integer $i_{\rm cold}$ denoting the innermost grid point in the cold state, and another integer $i_{\rm hot}$ giving the outermost grid point lying in the hot state. As in C93b and C94, we employ the thermal energy equation only for grid points such that $i_{\rm hot} < i < i_{\rm cold}$. For the radial extent of the front, $N_F = i_{\rm cold} - i_{\rm hot} - 1$.

The third panel of Figure 3 shows that, as the front propagates to smaller radii, N_F

decreases. This is mainly due to our grid spacing $\Delta r \propto \sqrt{r}$. The fractional width of the cooling front is always small compared to unity ($\sim$ 10 %), and unless many grid points are utilized, we overestimate the radial length scales associated with variations within the front. The values in Figure 3 and following figures are 50 day moving averages through the data, therefore the fact that $N_F < 1$ means that, on average, less than a single grid point defines the cooling front. During a majority of the time (for which $N_F < 1$) two adjacent grid points spanning the front are entirely in thermal equilibrium. The temperature at the inner point is decreasing only by virtue of the decrease in surface density associated with mass outflow across the hot/cold interface. Note the strong upturn in the $t_{\rm e-fold}$ curves associated with the times when N_F drops below unity. At this point, the cooling front is effectively prevented from having a region of strong variation which is narrower than the grid spacing, and we begin to underestimate dramatically the decay time. For the figures shown below we take $N = 1000$ grid points, unless otherwise stated. We note that previous studies of the accretion disk limit cycle model *used about 20-40 grid points to cover the entire disk*, and must have therefore considerably underresolved the fronts. The consequences of this underresolution will be addressed in the discussion section.

5.2.2. Effect of Varying Model Parameters

Figure 4 shows the effect of varying the exponent n in the $\alpha_0(h/r)^n$ law. The results shown in the second panel contain a major new result: for $n > 1.5$ the decay form is slower than exponential, while for $n < 1.5$ it is faster than exponential. The $n = 1.5$ curve is very close to exponential: $t_{\rm e-fold}$ varies by less than $\sim$ 10% after the initial (transient) configuration has been lost at $t \gtrsim 150$ days. (Although 150 days is comparable to the observed durations of outbursts in the BHXN, the departure from exponential decay in the models shown here is linear, so that once the transient ends we immediately begin to

see what the nature of the decay is. Therefore the specific duration of the transient is not relevant.) Much more importantly, the next few figures will show that the critical value $n = 1.5$ is independent of other parameters, such as the primary mass. Therefore, solely on the basis of the observed ubiquity of exponential decays, it would appear that one can infer $n \simeq 1.5$.

Note that there was a reflection of the cooling front at around $t = 320$ days in the $n = 1$ model. This re-triggering often happens, when the surface density profile left over in the cool state, behind a cooling front, is such that $\Sigma > \Sigma_{\rm max}$. If the two surface densities are comparable, then the exact triggering criterion can depend sensitively on details of the computation, such as the differencing scheme used in handling the advective terms (i.e., forward differencing, versus backward or mixed), and the number of grid points. For example, for $N = 600$, the $n = 1$ model does not show a re-triggering. On the other hand, one should not discount these heating front reflections as being entirely numerical. The over-buildup of surface density (relative to $\Sigma_{\rm max}$) behind the cooling front is a real, physical effect which may play a role in the observed secondary maxima. Without a great deal more testing, it is impossible to say just how much of this effect is numerical and how much is physical, therefore we would not want to make general claims about the nature of the secondary maxima based on these results.

Figure 5 shows the effect of varying the proportionality constant α_0 in the α scaling, while keeping all other parameters fixed. Here we use the optimal $n = 1.5$. The constant α_0 is varied by 0.3 dex between each curve. The second panel of Fig. 5 shows that $t_{\rm e-fold}$ is inversely proportional to α_0. (Note the re-triggering of an outburst in the $\log \alpha_0 = 2.0$ curve.) Figure 6 show the effect of varying the mass of the black hole, while keeping all other parameters fixed. We set $n = 1.5$ and $\log \alpha_0 = 1.7$. As in Fig. 5, there is a simple relation between $t_{\rm e-fold}$ and M_1 – here a direct proportionality instead of an inverse proportionality.

The $t_{\rm e-fold}$ curve for $M_1 = 5M_\odot$ begins to rise at $t \sim 300$ days due to the loss of resolution of the cooling front, and the $t_{\rm e-fold}$ curve for $M_1 = 20M_\odot$ shows a re-triggering at $t \sim 400$ days.

Figure 7 shows the effect of varying the outer disk radius, while keeping all other parameters fixed. This is equivalent to changing the orbital period of the system. Note in the first panel that the level of the rate of accretion onto the black hole increases with $r_{\rm outer}$. In the last section we saw that, for models in which α is constant, the mass of the stored gas varies roughly as the cube of the binary separation. For these models the increase is weaker because $\Sigma_{\rm max}(r)$ does not vary as strongly as r. From the second panel we see that the $e-$folding time scale for the decay is relatively insensitive to $r_{\rm outer}$. This is unfortunate in the context of the "Bailey relation" – an observed proportionality between $t_{\rm e-fold}$ and orbital period in the decay of the dwarf nova outbursts. This implies a nearly linear relation between $t_{\rm e-fold}$ and $r_{\rm outer}$, as first shown by Smak (1984). (As noted earlier, the $e-$folding times given in Tables 1-5 are not related to this $t_{\rm e-fold}$, because the outbursts in the previous section are not exponential.) One of the successes of the $\alpha \propto r^\epsilon$ scaling adopted by Cannizzo (1994) was that it could reproduce the Bailey relation. It is not immediately clear what the implications of this finding are. Perhaps the much smaller dynamic range in accretion disk radii for the dwarf novae changes the relation between $t_{\rm e-fold}$ and $r_{\rm outer}$ for the $\alpha_0(h/r)^n$ scaling from what we have inferred in this work. Future work must address this issue by testing the $\alpha_0(h/r)^n$ scaling for dwarf novae in a systematic fashion as was done by Cannizzo (1994).

6. The Width of the Transition Front

The physics associated with the nature of the decay – exponential versus non-exponential – is worth looking at in more detail. The form of the decay strongly depends on the velocity of the cooling transition front, which, in turn, depends on the width of the front. At the interface between the hot and cold state of the disk there is a very strong outflow of matter. The local mass flow rate under general, non-steady conditions, can be written as

$$\dot{M}(r) = 2\pi r v_r(r)\Sigma(r), \tag{5}$$

where the local flow velocity is

$$v_r(r) = -3\frac{\nu}{r}\left(2 + \frac{d\log\Sigma}{d\log r} + \frac{d\log T}{d\log r}\right), \tag{6}$$

where ν is the kinematic viscosity coefficient (Lin, Papaloizou, & Faulkner 1985). We adopt the convention that v_r and $\dot{M}$ are negative for inflow and positive for outflow. Matter flows outward across the cooling front and thereby allows the front to proceed inward, so the front speed is related to the flow speed by the ratio of surface densities on either side of the front. In traversing the cooling front to larger radii, Σ increases by $\sim 2-3$, but T decreases by ~ 10 – therefore the expression for the cooling front speed reduces approximately to

$$v_F \simeq \frac{3p\nu_F}{w}, \tag{7}$$

where $\nu_F = (2/3)\alpha_F h_F^2 \Omega_F$ is the viscosity coefficient evaluated in the hot state just interior to the cooling front, w is the width of the transition front determined by the radial length scale for variation in temperature T (Osaki 1989), and $p \sim 0.5$ is a factor which takes into account the piling up of material inside the cooling front (see eqn. [3.11] of CSW). Using

$\alpha_F = \alpha_0(h_F/r_F)^n$, $c_s = h_F\Omega_F$, and $p = 0.5$ gives

$$v_F \simeq \alpha_0 \frac{c_s^{n+2}}{(GM_1)^{(n+1)/2}} \frac{r_F^{(n+3)/2}}{w}. \tag{8}$$

We find numerically that c_s is constant with radius (see the uppermost dotted line in panel 2 of Fig. 2). In equation (8) we keep the cooling front width w as a general parameter.

What is the crucial property of the cooling front transition speed which determines whether or not the decay will be an exponential process? The answer to this question can be gleaned by careful consideration of the evolutionary sequences depicted in Figure 2 for a run tuned to produce exponential decay. In this context, by "exponential decay" we mean that the rate of accretion at the inner disk edge has an exponential form in time. Most of the mass flow of the gas lying in the hot region is outward mass flow at the cooling transition, however, and not mass accretion onto the central object. *The small, or consequential, mass loss at the inner edge is driven by the mass of gas in the hot state, and the mass of gas in the hot state is determined by the location of the interface between the hot and cool states – that is, by the location of the cooling front. Therefore, for the mass loss rate at the inner edge to decay exponentially with time, the mass of the hot disk must decay exponentially with time, the radius of the cooling front must decay exponentially with time, and the speed of the cooling front must decay exponentially with time.* Once this point has been appreciated, one can adopt the required form for the front speed $v_F \propto r_F$ in equation (8) and work backwards to find the front width w. Doing this using $n = 1.5$ gives $w = \sqrt{h_F r_F}$ – the cooling front width is the geometric average of the disk radius and the disk thickness (evaluated in the hot state just interior to the cooling front). This means that, for self-consistency, the width of the cooling front must in general be $\sqrt{h_F r_F}$.

This "postdiction" is easily verifiable with our high resolution runs. Figure 8 shows, on a log-log scale, the variation of the fractional front width w/r with radius as the cooling front moves inward, for the $n = 1.5$, $\log \alpha_0 = 1.7$ model. For comparison we show also $\sqrt{h/r}$

and h/r, where h is evaluated in the annulus just interior to the cooling front. The dotted curve shows the log of the number of grid points lying within the cooling front. At $\log r(\mathrm{cm}) \simeq 9$ we begin to lose numerical resolution, and the resulting slope $w/r \propto r^{-1/2}$ at smaller radii is caused by the grid spacing limitation $w \rightarrow \Delta r$, where $\Delta r \propto \sqrt{r}$. We numerically determine w by taking $r(i_{\mathrm{cold}}) - r(i_{\mathrm{hot}})$. From Fig. 8 we see that w/r closely follows $\sqrt{h/r}$ – i.e., $w = \sqrt{hr}$. We have also followed w/r for models in which (1) $n = 1$ and 2, (2) α varies in a step function between the low and high states (with no radial dependence), (3) different terms in the energy equation are set equal to zero (the two advective terms, and the radial viscous flux term), and (4) the dimensionless specific heat $c_p/(\mathcal{R}/\mu)$ is set equal to 2.5, and therefore not allowed to vary with partial ionization. *For all these runs w/r follows $\sqrt{h/r}$.*

Although we have not been able to derive this result from first principles, it appears to be a fundamental consequence of mass and angular momentum conservation, coupled with the fact that there is strong mass outflow in the vicinity of the cooling front. Figure 9 shows the evolution of the local flow speed and mass flux accompanying the $n = 1.5$ model. As noted earlier, the flow patterns result from local gradients in temperature and surface density. It is noteworthy that the relaxation to a lowest energy configuration, which the surface density diffusion equation always tries to enforce, leads to a flow pattern such that, for the inner region of the hot state disk where mass flow is inward, $\dot{M}$ is independent of radius, and for the outer region of the hot state disk where mass flow is outward, $\dot{M} \propto r^3$. (The exponent "3" here is quite approximate, given that the law only applies over a dynamic range of about a factor of 2 in radius.) The reason for this particular functional form is not now understood from first principles, but probably holds a clue to the explanation for $w = \sqrt{h_F r_F}$.

Previous workers have investigated the width of the front. The first consideration was

by Meyer (1984) who argued, by comparison with the width of combustion waves, that the front width is narrow, $w \simeq h$. Papaloizou & Pringle (1985, see also Meyer 1986) proposed a somewhat wider front, $w \simeq f^{1/2}h$, where $f \sim 3 - 10$ is a factor which takes into account the increased thermal time scale due to partial ionization effects. One might at first think, by considering Fig. 8, that our numerical results could be consistent with this if $f \sim 100$. This can be ruled out, however, from our experiments where we simplify the thermal energy equation and effectively set f to ~ 1. Furthermore, the functional form $w = \eta h$ would not have preferentially selected out $n = 1.5$ as being critical to exponential decay: equation (8) shows that the critical value would be 2 because $v_F \propto r_F^{n/2}$ for $w \propto h_F$. The next discussions of w appeared in papers which quoted numerical results. For example, CSW looked at previous computations showing the surface density and temperature evolution and noted that $w/r \sim 0.1$, independent of radius (see also p. 333 of Mineshige 1987 and p. 56 of Mineshige & Shields 1990). From Fig. 8 we see that this is roughly accurate, and indeed, for the dwarf nova disks which had mainly been considered previously, the small dynamic range in disk radius was such that the variation of w/r with r would have been minimized and therefore not particularly noticeable in the computations. Again, however, our results clearly exclude this relation for w. Also, if w were to vary as r, then, from equation (8), $n = 1$ would be required to produce exponential decays because, for $w \propto r_F$, we see that $v_F \propto r_F^{(n+1)/2}$.

7. Discussion

We have presented the results of an investigation of the gross features involved in the accretion disk limit cycle model for outbursts in the BHXN employing two types of scalings for the viscosity parameter – $\alpha \propto r^\epsilon$ and $\alpha \propto (h/r)^n$. In the former models we utilize a step function variation between α in the low and high states, whereas for the latter we do not.

Using the latter scaling, we are unable to execute the operation of the model by utilizing the local maximum in the $\log T_e - \log \Sigma$ curves which is due to the convective effect. Without the ad hoc jump in α, there is too little variation in the vertically integrated stress W between $\Sigma_{\rm max}$ and $\Sigma_{\rm min}$. We must therefore utilize the local maximum produced by the opacity effect. The midplane temperature at $\Sigma_{\rm max}$ for this feature is substantially less (see the "$T_{\rm mid}$" column in Table 2 of Cannizzo & Wheeler 1984), and therefore the contrast in W between $\Sigma_{\rm max}$ and $\Sigma_{\rm min}$ is greater.

As regards the propagation of the cooling front, we find that a self-regulating mechanism operates to ensure that $w/r = \sqrt{h_F/r_F}$, where the subscript "F" refers to the hot state of the disk just interior to the cooling front. This corresponds to the local minimum in the $S-$curve. Given that the front speed is $v_F = \nu_F/w$, this gives $v_F \simeq \alpha_F (h_F/r_F)^{3/2} \Omega_F r_F = \alpha_F c_s (h_F/r_F)^{1/2}$, where c_s is the sound speed in the hot state.

We have detailed the cause for the exponential decay of the X-ray flux. The reason for the decay is the exponential decay of the mass of gas comprising the hot state, which is controlled by the location of the cooling front which divides the hot and cold states. Thus, for exponential decay we require v_F $(= dr_F/dt) \propto r_F$. Given that (1) $v_F \simeq \alpha_F (h_F/r_F)^{3/2}$ $\Omega_F r_F$, (2) $h^2\Omega^2 = \mathcal{R}T/\mu$ (from hydrostatic equilibrium), and (3) the temperature at the lower bend in the S-curve, or, equivalently, in the hot disk just interior to the cooling front, T_F, is independent of radius, we see that for $n = 1.5$ we obtain $v_F \propto r_F$. Previous studies noted that $w > h$, but cast w either in terms of h (i.e., $w \sim \eta h$ where $\eta \sim 1 - 10$), or in terms of r (i.e., $w \sim \chi r$ where $\chi \sim 0.1$). Our finding of the relation between the character of the decay of the bolometric flux and n led us to use our high resolution code to search for a $w = f(h,r)$ dependence. We believe the relation $w = \sqrt{hr}$ to be universal: our tests have shown this to be independent of the way in which the input physics is parametrized.

In summary, using $w = \sqrt{h_F r_F}$ gives, as the general expression for the cooling front speed,

$$\dot{r}_F \simeq -\alpha_0 c_s^{n+3/2} \left(\frac{r_F}{GM_1}\right)^{(2n+1)/4}, \tag{9}$$

where $\alpha = \alpha_0 (h/r)^n$ and $c_s = \sqrt{\mathcal{R} T_F / \mu_F}$.

In this work we have paid particular attention to systematic effects in the modeling which must be addressed in order to assess the reliability of the model and to understand how trustworthy are the restrictions we place on the allowable input physics. We find, for instance, that of order $N \simeq 1000$ grid points are required to cover adequately the dynamic range in disk radii which must be spanned for this problem. We are able to use such a large number for the $\alpha \propto (h/r)^n$ scaling taking $r_{\rm inner} = 10^7$ cm because our explicit code requires $O(N)$ operations per time step, whereas an implicit code requires $O(N^2)$ because of the grid matrix inversions. This comes about because, in an explicit code, the updated values of the physical quantities at a given grid point are determined by spatial differences of values taken at the previous time step, whereas in an implicit code, the values used in the spatial differences are those from the following time step. Therefore, in solving a diffusion equation for instance, one must invert a tridiagonal system of equations using the implicit method (Press et al. 1986). For the explicit method, one merely computes the small changes in the variables at each grid point and adds them to the previous values.

Furthermore, by taking a small time step and a large N in our explicit code we are able to follow very fine scale structure within the transition fronts and thereby determine more accurately the front speeds. How do our findings regarding the exponential decay relate to previous studies? From our experiments where we vary n, we expect $n = 0$ models to give faster-than-exponential decays. Huang & Wheeler (1989), for example, look at models for A0620-00 in which α varies in a step function between the low and high states. Their Figure 3 giving the decline of the B band flux shows the expected faster-than-exponential drop-off (see also Fig. 13 of Cannizzo 1993b). The most systematic study to date which

has explored the limit cycle mechanism in the BHXN is that of Mineshige & Wheeler (1989). This study utilized an implicit code and took $N = 21$ grid points to cover a disk which spans a dynamic range of 10^4 from inner to outer edge. Thus, in their modeling, $\log(r_{i+1}/r_i) = \log(r_{\rm outer}/r_{\rm inner})/(N-1) = 4/20$, or $r_{i+1}/r_i \simeq 1.6$ for all grid points i, giving $\Delta r/r = (r_{i+1} - r_i)/[(r_{i+1} + r_i)/2] \simeq 0.45$. This is clearly inadequate to resolve structure on a scale $\delta r/r \approx 0.1$. Mineshige & Wheeler note that there is no change in their computations upon doubling N to 41 grid points. This is expected since they are still well within the grid spacing-dominated regime. Given this, it seems likely that their transition front widths were underresolved, and that the decay rates in their models were limited by their grid spacing. The underresolution is tempered somewhat by the fact that their logarithmic grid spacing in which $\Delta r/r$ is constant is more ideally suited to the natural decrease in front width with decreasing radius than is our spacing in which $\Delta r/r$ varies as $1/\sqrt{r}$. If one desired, say, ~ 5 resolution elements within the front using the grid spacing in which $\Delta r/r$ is constant, this would require $\Delta r/r \approx 0.02$, necessitating the use of $N \approx 465$ grid points (i.e., $10^{4/465} \approx 1.02$). Mineshige & Wheeler (1989) considered models using the $\alpha \propto (h/r)^n$ scaling for $0.5 \leq n \leq 2.5$. There is a slight variation in the degree of concavity of the light curve decay shape as n was made to vary in their models. Mineshige & Shields (1990) used the same code as that described in Mineshige & Wheeler (1989) and noted that, as regards the decay, $v_F \propto r_F$ for $n = 1$. This is understandable if their transition front widths were limited by their grid spacing. In that case $w \rightarrow \Delta r$, and, since they adopt a logarithmic grid spacing $\Delta r \propto r$, this means that w was constrained in their models to vary as r, and could not vary as $\sqrt{hr}$. From equation (8) we see that this would spuriously select $n = 1$ as being the critical value for exponential decay because $v_F \propto r_F^{(n+3)/2}/w$: if $w \propto r_F$, we see $v_F \propto r_F^{(n+1)/2}$. This accounts for the fact that one still sees variations in the degree of concavity of the decay of the light curve even in computations for which $w \propto r_F$ is artificially imposed by the numerics. More recently Ichikawa et al. (1994) have examined

the possible implications of applying Osaki's thermal-tidal instability to the black hole binaries. It is difficult to carry out a meaningful comparison of our results with theirs, given that their model has approximately ten free parameters which can be adjusted. Nevertheless, one possibly important piece of physics noted by Ichikawa et al. which might affect the decay rate is a variable outer disk radius. Future work must address this issue.

In our models we use the observed exponential decay of the X-ray flux in the BHXN to strongly constrain n to be 1.5. This constraint appears to be robust in the sense that it does not depend on systematic effects such as our particular characterization of the steady state physics (as long as α can indeed be parametrized as $\sim (h/r)^n$). If n differs from 1.5 by more that $\sim 10\%$ we see a noticeable deviation from $t_{\rm e-fold}$ being constant over, for example, a $\sim$200 day time span – a length of time during which $t_{\rm e-fold}$ was observed to be constant in A0620-00, GRO J0422+32, and GS2000+25. Furthermore, from the observed value of $t_{\rm e-fold}$ of $\sim$ 30 days (MYI) we can infer $\alpha_0 \sim 10^{1.7}$ (for the $\alpha = \alpha_0(h/r)^n$ law). The constraint on this constant is less secure than the one on n because there are systematic effects in the model which can affect the rate of decay but not the functional form of the decay (i.e., exponential versus non-exponential). These systematic effects include such factors as the precise scalings used to characterize the S-curve, and the finite differencing scheme used in discretizing the disk equations.

In our models with $\alpha = \alpha_0(h/r)^{1.5}$, we find that $t_{\rm e-fold}$ determined from the rate of accretion onto the compact object depends to the same degree on α_0 and M_1 – an inverse proportionality for the former parameter and a direct proportionality for the latter. This also comes directly from the previous relation for v_F. Taking $n = 1.5$ in equation (9) gives

$$\frac{dr_F}{dt} \simeq -\frac{\alpha_0}{GM_1}\left(\frac{\mathcal{R}T_F}{\mu_F}\right)^{1.5} r_F, \tag{10}$$

where $T_F = 30,000$ K is the midplane temperature of the gas just interior to the cooling front radius r_F. So the $e-$folding time for r_F is $t_{\rm e-fold}(r_F) \equiv (-d\ln r_F/dt)^{-1} = (GM_1/\alpha_0)c_s^{-3}$,

where $c_s \simeq 16$ km s^{-1}. From eqn. (4) we see $c_s \propto \sqrt{T_{\rm min}}$ varies roughly as $r^{-0.025}$. The mass of the hot gas enclosed by the cooling front at a given time varies roughly as $r_F^{2.6}$, so $t_{\rm e-fold}(\dot{M}_{\rm inner}) \equiv (-d \ln \dot{M}_{\rm inner}/dt)^{-1} \simeq t_{\rm e-fold}(r_F)/2.6$. Using the observed value of ~ 30 days for the $e-$folding decay time for the X-ray flux, and, assuming a $\sim 10 M_\odot$ accretor, gives $\alpha_0 \simeq 50$, in agreement with our numerical results. The law $\alpha = 50(h/r)^{1.5}$ is the same as that employed by Meyer & Meyer-Hofmeister (1984) in their time dependent study of dwarf nova outbursts. The fact that $t_{\rm e-fold} \propto M_1/\alpha_0$ is interesting in view of the fact that the observed $e-$folding times for BHXN are all $\sim 30 - 50$ days (MYI). If we view α_0 as a universal constant, then the spread in the observed decay rates must be due to the spread in black hole masses. (MYI noted also that, in their simplified decay model, the decay time varies as M_1/α_0. This coincidence with our findings appears to be fortuitous, given the fact that their decay time scaling depends only on the standard viscous time scale and does not take into account the properties of the cooling flow.) The only shortcoming of the $(h/r)^n$ law appears to be that there is no sensitivity of $t_{\rm e-fold}$ on $r_{\rm outer}$ (or, equivalently, $P_{\rm orbital}$) as is required in the Bailey relation for dwarf novae (Smak 1984, Cannizzo 1994). Nevertheless, it is interesting that a simple scaling of our $t_{\rm e-fold}$ to dwarf nova parameters (i.e., $M_1 \sim 1 M_\odot$) gives a reasonable number, i.e., $t_{\rm e-fold} \sim 3$ days.

As we have sought in this work to understand the most basic attributes of the BHXN, we have not addressed the question of the secondary maxima, nor the issue of disk irradiation. However, in addition to the disk instability computations discussed previously we have also looked at the situation where there is no S-curve in $\log T_e - \log \Sigma$ but rather a monotonic $\Sigma - T_e$ relation. This could correspond either to the class of models promulgated by Hameury, King, & Lasota (1986, 1987, 1988), or to the situation in which irradiation of the accretion disk is so strong that the cooling front is unable to propagate (Tuchman, Mineshige, & Wheeler 1990, Mineshige, Tuchman, & Wheeler 1990). The absence of a cooling front means that the decay of X-ray flux in an outburst can proceed only by

the gradual accretion of stored disk matter onto the central object. This long standing problem has been looked at by many investigators and, it has been shown for a variety of assumptions, that power law decays occur rather than exponential decays (e.g., Mantle & Bath 1983, Lyubarskii & Shakura 1987, Cannizzo, Lee, & Goodman 1990, MYI). The reason for this can be seen by considering the diffusion equation for surface density in which the time rate of change of Σ is a function of radial derivatives of $\nu\Sigma$, where ν is the kinematic viscosity coefficient $(2/3)(P/\rho)(\alpha/\Omega)$. The solution to the diffusion equation can only assume an exponential form – $\Sigma = \Sigma_0 e^{-t/t_e}$ – if ν is independent of local physical conditions in the disk. For $P_{\rm gas} > P_{\rm radiation}$ we see that $\nu \propto \alpha T$. In order to offset the natural variation of ν with T which is inherent in the $\alpha-$model, we must invoke $\alpha \propto T^{-1}$. Hydrostatic equilibrium gives $P/\rho \simeq \Omega^2 h^2$, so this constraint is equivalent to requiring $\alpha = \alpha_0 (h/r)^n$ with $n \simeq -2$ in order to get an exponential decay of the luminosity with a hot disk.

With α_0 and n constrained by the observed X-ray decays, and M_1, $r_{\rm inner}$, and $r_{\rm outer}$ constrained by the known systemic parameters, we have exhausted our supply of adjustable parameters. In our "standard model" for the section where $\alpha = f(r)$ we produce outbursts which have a long plateau preceding the exponential decay. This feature was shown to be a success of the model in accounting for the long term behavior of SS Cyg: a dwarf nova showing alternating long and short outbursts – the long outbursts possessing a plateau at maximum which precedes the faster, exponential decay. Although some BHXN show plateaus, the brightest and best studied ones have much shorter plateaus or no plateaus. In A0620-00, for instance, the plateau was about a week long for the 1975 outburst. To avoid producing the plateaus and to preserve α_0 and n, we must somehow get rid of a large fraction of the disk during the early stages of the outburst. There may be support for this idea with the recent radio observations of mass ejection during the outbursts in some BHXN (Mirabel & Rodriguez 1994, Tingay et al. 1995, Hjellming 1995). It is interesting

that, at the beginning of an outburst the stored disk mass is roughly 4×10^{25} g in our "standard model", and the ejecta mass inferred by Mirabel & Rodriguez is $\sim 2 \times 10^{25}$ g. The disk mass could conceivably be ejected through radiation pressure during the early, near-Eddington phase of accretion. On the other hand, in this paper we have not run models using the $\alpha = g(h/r)$ law which progress through the complete cycle of outburst and quiescence, therefore we do not know whether, for the default parameters used in the $\alpha = g(h/r)$ section, the outbursts will be flat-topped. Based on the fact that $\Sigma_{\rm max}/\Sigma_{\rm min}$ is smaller for the $\alpha = g(h/r)$ models than for the $\alpha = f(r)$ models, the light curves may go directly into the exponential decay phase immediately after the period of rising light has ended.

Throughout this study our guiding principle has been to attempt to reproduce the exponential decay for outbursts. Not all systems, however, exhibit this behavior. The most notable exception is V404 Cygni, which was discovered in outburst by Ginga on 23 May 1989. There were large variations seen in the X-ray flux during the early stages of the outburst – sporadic bursts during which the flux varied by $\sim 10 - 100$ over minutes to hours (Terada et al. 1994). Most interesting, however, was the fact that *the subsequent, long-term decrease in flux as the outburst faded followed a power-law form in time, not an exponential.* This was seen in the X-ray, optical, and radio bandpasses (Han & Hjellming 1992). V404 Cyg also has by far the longest orbital period of those for which periods have been determined. We propose the following scenario to account for the combination of power-law decay in a system with such a long orbital period. We showed earlier that the mass of gas stored in quiescence varies very roughly as the cube of the orbital separation. The peak luminosities for the outbursts computed in this work, modeled to be in systems characteristic of A0620-00 where $P_{\rm orbital} \simeq 8$ hrs, are of order $0.1 L_{\rm Edd}$. If we increase $P_{\rm orbital}$ dramatically, then, as the very large mass stored in the disk during quiescence begins to flow onto the central black hole during the onset of instability, it

quickly reaches the Eddington limit, at which point the thin disk approximation used in this study breaks down and accretion becomes quasi-spherical. During the transition stage from disk accretion to spherical accretion there may be violent variations in the central flux due to non-axisymmetric instabilities in the flow. If the spin to mass ratio J/M is large for V404 Cyg, the Lense-Thirring effect would tend to redirect gas elements which approach the black hole on orbits out of the binary orbital plane into orbits which are more nearly coplanar with the surface orthogonal to the black hole spin vector. At the points of intersection between these elements and other parts of the disk there would be strong shocks. This would continue as more and more of the material which had been stored at large radii during quiescence continued to move to smaller radii. Support for this general picture can be found by examining the X-ray spectral evolution of the outbursts. For most of the systems – those mentioned earlier with $P_{\rm orbital} \simeq 10$ hrs – one sees a soft component at early times which is most likely produced by a standard, geometrically thin and optically thick disk. As the outburst fades, the spectrum inevitably becomes harder and approaches a power law which is thought to be produced by hot, optically thin gas. In V404 Cyg, however, the soft component was never seen, indicating that a hot, optically thick disk was unable to form. (Compare figures 4 and 10 in Tanaka 1989 showing GS2000+25 – a system with an exponentially decaying outburst – and V404 Cyg). Against this picture, however, we must add that GRO J0422+32, with a relatively short orbital period of ~ 5 hrs, also showed only a hard spectrum during its outburst.

8. Conclusions

We have presented the results of a parameter study of the limit cycle mechanism to account for outbursts in the X-ray novae. The basic observation defining the characteristics of the outbursts in the X-ray flux of the brightest and most well studied systems are a fast

rise, followed by an exponential decay with a time constant of 30 to 60 days.

Light curves for outbursts using the scaling $\alpha \propto r^{\epsilon}$ taking $\alpha_{\rm hot}/\alpha_{\rm cold} = 10$ show a slow rise (i.e., $\sim$ 50 days), followed by a long plateau stage, and then a very rapid, faster than exponential decay. We have delineated the effects on the outburst properties by varying the input parameters of the model in a controlled way.

Our runs with $\alpha \propto (h/r)^n$ produced several interesting results.

(1) On the numerical side, for the grid spacing $\Delta r \propto \sqrt{r}$, we find that $O(1000)$ grid points must be used in the modeling for our assumed dynamic range in disk radii of $\sim 10^4$. Fewer points leads to an inadequate resolution of the cooling front and an over-estimate of the decay time scales. Studies which take $O(20)$ grid points may be entirely limited by their grid spacing. The grid spacing $\Delta r \propto r$ used in these works, however, is more expeditious for following the movement of transition fronts, and they would have required $\sim 400 - 500$ grid points to obtain a resolution in which about 5 grid points lie within the cooling front at all radii.

(2) Numerically we find the cooling front width to be the geometric average of h and r, evaluated in the hot state just interior to the cooling front. This leads to a cooling front speed $v_F = \alpha_F (h_F/r_F)^{3/2} \Omega_F r_F$. This result does not depend on how we parametrize the physics of the accretion disk. It appears to be a fundamental consequence of having an abrupt drop in the viscosity at some radius which induces a strong outflow.

(3) We constrain n to be 1.5 ± 0.1 based on the exponential form of the decay. This constraint appears to be robust in that it is independent of the other parameters in the model. The value 1.5 is selected because, for a front width $w = \sqrt{hr}$, this law leads to $v_F \propto r_F$. If w had varied as r the critical value for n would have been 1, and if w had varied as h the critical value for n would have been 2. These dependencies come about because,

for $w \propto r_F$, equation (8) gives $v_F \propto r_F^{(n+1)/2}$, whereas for $w \propto h_F$, we get $v_F \propto r_F^{n/2}$. For models with the correct dependence $w = \sqrt{h_F r_F}$, we find $v_F \propto r_F^{(2n+1)/4}$.

(4) For the class of models in which $n = 1.5$, we derive the relation for the $e-$folding decay time for the X-ray flux $t_{\rm e-fold} \simeq 0.38(GM_1/\alpha_0)c_s^{-3}$, where $c_s \simeq 16$ km s^{-1}. By assuming a $\sim 10M_\odot$ accretor in the BHXN, we constrain α_0 to be $\sim 10^{1.7}$ based on the observed ~ 30 day time scale for the exponential decay of X-ray flux.

(5) If the cooling front is unable to propagate, and thus there is effectively a monotonic relation between T_e and Σ in the steady state physics, then $n \simeq -2$ is required for exponential decays. While some X-ray reprocessing is probably required to produce the level of the optical flux observed in at least some systems (e.g., Cheng et al. 1992), the irradiation of the disk cannot be so great as to affect significantly the steady state scalings (as discussed in Tuchman et al. 1990).

Figure 1 of Ko & Kallman (1991) shows schematically two ways in which X-rays from the accreting object can irradiate the disk. In their drawing, the disk is flared, in line with the conventional Shakura & Sunyaev "outer disk" for which $h/r \propto r^{0.125}$. This assumes, however, that $\dot{M}(r)$ is constant. Fig. 2b of Cannizzo (1994) shows that this is not true for accretion disks containing a cooling front. In fact, h/r decreases with r so that the outer disk is shielded from direct irradiation by the central source. Thus, even with irradiation included, the cooling front should still be able to propagate. A more delicate issue is that of reprocessing X-ray flux scattered from a corona overlying the disk. The efficacy of such a process depends on assumptions made regarding the corona.

One of the goals of accretion disk research has been to constrain the viscosity – either its magnitude or functional form. The value $\alpha = 50(h/r)^{1.5}$ may prove to be the long-sought universal form. Meyer & Meyer-Hofmeister (1984) used exactly this same function in their time dependent modeling of dwarf novae, systems with $\sim 1M_\odot$ accretors. Huang &

Wheeler's (1989) results seemed to provide evidence that α may have to be lower in the BHXN than it is in dwarf novae if the limit cycle model is to work. Our results have failed to confirm this. It appears that $\alpha = 50(h/r)^{1.5}$ can work for both types of systems. The only way to test this assertion will be to run parallel sets of computations on both types of systems *using the same code* so as to negate systematic numerical differences between codes. If there is one function for α that applies to all accretion disks, then the longer time scales associated with the outbursts in the BHXN may be due to the fact that, in going from dwarf novae to BHXN, M_1 is much larger and ζ is much smaller. If α is constant, the $e-$folding decay time varies with M_1 as we have shown, and the recurrence time varies inversely with ζ (CSW).

The study of just the decay of outbursts has proven in this work to be sufficiently interesting that we chose not to follow the disk instability through several complete cycles in order to investigate the rise times and recurrence times. That is the next obvious step, and work is underway to do this. Now that we no longer have the freedom to vary α as desired (e.g., Ichikawa et al. 1994), the results of such a study will be especially interesting and should allow us to constrain the efficacy of mechanisms external to the standard limit cycle model which might alter the surface density distribution during quiescence, such as some evaporation process (e.g., Meyer & Meyer-Hofmeister 1994, Narayan, McClintock, & Yi 1996). Such mechanisms have the potential to affect the rise times and recurrence times for outbursts.

We thank the following people for allowing us generous use of CPU time on their DEC AXP workstations: C. Hughes and G. Sonneborn (Goddard Space Flight Center); A. Saha, J. Krist, L. Taff, and B. Zellner (Space Telescope Science Institute). We also thank Craig Wheeler, Jim Pringle, Shin Mineshige, and Jean-Pierre Lasota for useful criticisms. JKC was supported by the National Academy of Sciences through a National Research

Council associateship in the Laboratory for Astronomy and Solar Physics at Goddard Space Flight Center, and through the visiting scientist program under the Universities Space Research Association (USRA contract NAS5-32484) in the Laboratory for High Energy Astrophysics at Goddard Space Flight Center. ML acknowledges support from NASA grants NAGW-2678, GO-5499, and GO-4377 at the Space Telescope Science Institute.

REFERENCES

Armitage, P. J., Livio, M., & Pringle, J. E. 1995, ApJ, in press

Bailyn, C., Orosz, J., McClintock, J., & Remillard, R. 1995, IAU Circ., 6173

Balbus, S. A., & Hawley, J. F. 1991, ApJ, 376, 214

Bath, G. T., & Pringle, J. E. 1982, MNRAS, 199, 267

Cannizzo, J. K. 1992, ApJ, 385, 94

Cannizzo, J. K., 1993a, in Accretion Disks in Compact Stellar Systems, ed. J. C. Wheeler (Singapore: World Scientific), p. 6

Cannizzo, J. K. 1993b, ApJ, 419, 318

Cannizzo, J. K. 1994, ApJ, 435, 389

Cannizzo, J. K., Lee, H. M., & Goodman, J. 1990, ApJ, 351, 38

Cannizzo, J. K., Shafter, A. W., & Wheeler, J. C. 1988, ApJ, 333, 227

Cannizzo, J. K., & Wheeler, J. C. 1984, ApJS, 55, 367

Cannizzo, J. K., Wheeler, J. C., & Ghosh, P. 1982, in Pulsations in Classical and Cataclysmic Variable Stars, ed. J. P. Cox & C. J. Hansen (Boulder: Univ. Colorado Press), 13

Cannizzo, J. K., Wheeler, J. C., & Ghosh, P. 1985, in Proc. Cambridge Workshop on Cataclysmic Variables and Low-Mass X-ray Binaries, ed. D. Q. Lamb & J. Patterson (Dordrecht: Reidel), 307

Casares, J., Charles, P. A., & Naylor, T. 1992, Nature, 355, 614

Charles, P. A., & Casares, J. 1995, IAU Circ., 6193

Chen, W., Livio, M., & Gehrels, N. 1993, ApJ, 408, L5

Cheng, F. H., Horne, K., Panagia, N., Shrader, C. R., Gilmozzi, R., Paresce, F., & Lund, N. 1992, ApJ, 397, 664

Ebisawa, K., et al. 1994, PASJ, 46, 375

Eracleous, M., Halpern, J., & Patterson, J. 1991, ApJ, 382, 290

Faulkner, J., Lin, D. N. C., & Papaloizou, J. C. B. 1983, MNRAS, 205, 359

Gottlieb, E. W., Wright, E. L., & Liller, W. 1975, ApJ, 195, L33

Hameury, J. M., King, A. R., & Lasota, J. P. 1986, A&A, 162, 71

Hameury, J. M., King, A. R., & Lasota, J. P. 1987, A&A, 171, 140

Hameury, J. M., King, A. R., & Lasota, J. P. 1988, A&A, 192, 187

Han, X., & Hjellming, R. M. 1992, ApJ, 400, 304

Hawley, J. F., Gammie, C. F., & Balbus, S. A. 1995, ApJ, 440, 742

Hjellming, R. M. 1995, Nature, submitted

Huang, M., & Wheeler, J. C. 1989, ApJ, 343, 229

Ichikawa, S., Mineshige, S., & Kato, T. 1994, ApJ, 435, 748

Ichikawa, S., & Osaki, Y. 1992, PASJ, 44, 15

Ko, Y.-K., & Kallman, T. R. 1991, ApJ, 374, 721

Lasota, J. P. 1995, in IAU Symposium 165, Compact Stars in Binaries, ed. van den Heuvel, E.P.J., et al., in press.

Lin, D. N. C., Papaloizou, J., & Faulkner, J. 1985, MNRAS, 212, 105

Livio, M. 1994, in 22nd Saas Fée course, Interacting Binaries, ed. H. Nussbaumer, & A. Orr (Berlin: Springer-Verlag), p. 135

Ludwig, K., Meyer-Hofmeister, E., & Ritter, H. 1994, A&A, 290, 473

Lyubarskii, Yu. É., & Shakura, N. I. 1987, Soviet Astron. Lett., 13, 386

Mantle, V. J., & Bath, G. T. 1983, MNRAS, 202, 151

Martin, A. C., Casares, J., Charles, P. A., van der Hooft, F., & van Paradijs, J. 1995, MNRAS, 274, 46P

McClintock, J. E., Horne, K., & Remillard, R. A. 1995, ApJ, 442, 358

McClintock, J., Petro, L. D., Remillard, R. A., & Ricker, G. R. 1983, ApJ, 266, L27

McClintock, J., & Remillard, R. A. 1986, ApJ, 308, 110

Meyer, F. 1984, A&A, 131, 303

Meyer, F. 1986, MNRAS, 218, 7P

Meyer, F., & Meyer-Hofmeister, E. 1981, A&A, 104, L10

Meyer, F., & Meyer-Hofmeister, E. 1983, A&A, 128, 420

Meyer, F., & Meyer-Hofmeister, E. 1984, A&A, 132, 143

Meyer, F., & Meyer-Hofmeister, E. 1994, A&A, 288, 182

Mineshige, S. 1987, Ap&SS, 130, 331

Mineshige, S., & Osaki, Y. 1983, PASJ, 35, 377

Mineshige, S., & Shields, G. A. 1990, ApJ, 351, 47

Mineshige, S., Tuchman, Y., & Wheeler, J. C. 1990, ApJ, 359, 176

Mineshige, S., & Wheeler, J. C. 1989, ApJ, 343, 241

Mineshige, S., Yamasaki, T., & Ishizaka, C. 1993, PASJ, 45, 707

Mirabel, I. F., & Rodriguez, L. F. 1994, Nature, 371, 46

Mukai, K., & Shiokawa, K. 1993, ApJ, 418, 863

Narayan, R., McClintock, J. E., & Yi, I. 1996, ApJ, 457, in press

Narayan, R., & Yi, I. 1995, ApJ, 452, in press

Osaki, Y. 1989, in Theory of Accretion Disks, ed. F. Meyer, W. J. Duschl, J. Frank, & E. Meyer-Hofmeister (Kluwer: Dordrecht) p. 183

Papaloizou, J. C. B., & Pringle, J. E. 1985, MNRAS, 217, 387

Pojmański, G. 1986, Acta Astr., 36, 69

Press, W. H., Flannery, B. P., Teukolsky, S. A., & Vetterling, W. T. 1986, Numerical Recipes (New York: Cambridge Univ. Press)

Pringle, J. E., Verbunt, F., & Wade, R. A. 1986, MNRAS, 221, 169

Remillard, R. A., McClintock, J. E., & Bailyn, C. D. 1992, ApJ, 399, L145

Shakura, N. I., & Sunyaev, R. A. 1973, A&A, 24, 337

Smak, J. 1983, ApJ, 272, 234

Smak, J. 1984, Acta Astr., 34, 161

Tanaka, Y. 1989, in Proc. 23rd ESLAB Symposium (ESA SP-296), vol. 1, ed. J. Hunt, B. Battrick (ESA: Noordwijk), 3.

Terada, K., Miyamoto, S., Kitamoto, S., & Egoshi, W. 1994, PASJ, 46, 677

Tingay, S. J., et al. 1995, Nature, 374, 141

Tuchman, Y., Mineshige, S., & Wheeler, J. C. 1990, ApJ, 359, 164

van Paradijs, J., & Verbunt, F. 1984, in AIP Conf. Proc. 115, High Energy Transients in Astrophysics, ed. S. E. Woosley (New York: AIP), 49

Vishniac, E. T., & Diamond, P. 1992, ApJ, 398, 561

Vrtilek, S. D., Penninx, W., Raymond, J. C., Verbunt, F., Hertz, P., Wood, K., Lewin, W. H. G., & Mitusda, K. 1991, ApJ, 376, 278

Wagner, R. M., Starrfield, S. G., Hjellming, R. M., Howell, S. B., & Kreidl, T. J. 1994, ApJ, 429, L25

White, N. E., Kaluzienski, J. L., & Swank, J. H. 1984, in AIP Conf. Proc. 115, High Energy Transients in Astrophysics, ed. S. E. Woosley (New York: AIP), 31

This manuscript was prepared with the AAS LaTeX macros v3.0.

FIGURE CAPTIONS

Figure 1. A collection of light curves of runs in which α varies as r^{ϵ}, where here $\epsilon =$ 0., 0.1, 0.2, 0.3, 0.4, and 0.5. The curves for larger ϵ decay more slowly. For $\epsilon = 0.4$ and 0.5, there are several retriggerings of the heating front before the final decay to quiescence begins. For all runs shown here and described earlier, the outbursts have a flat-topped plateau portion and faster than exponential form. Thus these parameters cannot reproduce the light curves for the systems such as A0620-00, Nova Muscae, J0422+32, and GS2000.

Figure 2. The evolution of surface density Σ, midplane temperature T, and viscosity parameter α, as functions of radius during the decay of an outburst. The initial condition for which $\Sigma(r) = 0.95\Sigma_{\rm max}(r_{\rm outer})\ (r/r_{\rm outer})^{-3/4}$, is shown by the dashed curve. The dotted curves show the conditions associated with $\Sigma_{\rm max}$ and $\Sigma_{\rm min}$. We take $r_{\rm inner} = 10^7$ cm, $r_{\rm outer} = 1.5 \times 10^{11}$ cm, $M_1 = 10M_\odot$, $\alpha = 10^{1.7}(h/r)^{1.5}$, and $N = 1000$. These parameters define our "standard model" for the $\alpha \propto (h/r)^n$ law and are used by default in the following figures, unless stated otherwise. Each curve is separated by 100 days of evolution. As time increases the cooling transition front which marks the interface between the hot and cold states advances to smaller radii, and the values of Σ, T, and α in the inner regions of the disk become smaller as material flows outward across the hot/cold interface and augments the mass of the outer, cold disk.

Figure 3. The effect on the decay of an outburst of varying the number of grid points. The initial condition is as in Fig. 2. We show four curves representing $N = 300$, 500, 700, and 1000. The first panel shows the rate of accretion at the inner disk edge onto the central black hole, in g s^{-1}. The Eddington rate of accretion onto a $\sim 10M_\odot$ black hole is $\sim 10^{19}$ g s^{-1}, assuming a rest mass-to-energy conversion efficiency of $\sim 10\%$. The second panel shows the 50 day moving averages of the locally defined ϵ–folding timescale (in days) from each of the curves in the first panel. The third panel shows the 50 day moving averages of the

number of grid points that lie inside the cooling front. As N increases we are better able to resolve fine scale structure within the cooling front, and $t_{\rm e-fold}(t)$ approaches a limiting (constant) value. During the later stages of evolution where $N_F < 1$, we see a systematic rise in $t_{\rm e-fold}$ due to underresolution of the cooling front.

Figure 4. The effect of varying the exponent n in the scaling $\alpha = \alpha_0(h/r)^n$. In this and subsequent models we take $N = 1000$. The parameters are the same as before, with the third panel now showing the cooling front speed (in units of km s^{-1}) determined by following the movement of $r(i_{\rm hot})$ – the outermost radial point at any given time which is in thermal equilibrium on the upper stable branch of solutions. To keep the values for $t_{\rm e-fold}$ in a common range, we adjust α_0 for each run: for $n = 1$, $\alpha_0 = 10^{0.7}$; for $n = 1.5$, $\alpha_0 = 10^{1.7}$; and for $n = 2$, $\alpha_0 = 10^{2.7}$. From the second panel we see that the law $\alpha \propto (h/r)^1$ gives a faster-than-exponential decay (i.e., $t_{\rm e-fold}$ decreasing with time), the law $\alpha \propto (h/r)^2$ gives a slower-than-exponential decay (i.e., $t_{\rm e-fold}$ increasing with time), and the law $\alpha \propto (h/r)^{1.5}$ gives close to an exactly exponential decay (i.e., $t_{\rm e-fold}$ constant). Note that the $n = 1.5$ curve is the same as the $N = 1000$ curve in Fig. 3.

Figure 5. The effect of varying the proportionality constant α_0. The parameters are the same as before (i.e., $n = 1.5$, $M_1 = 10M_\odot$, and $N = 1000$), and the small numbers beside each curve give $\log \alpha_0$. The cooling front reflects into a heating front at $t \simeq 140$ days in the $\log \alpha_0 = 2.0$ curve. The heating front moves outward until $t \simeq 180$ days, at which time it is again reflected inward as a cooling front. The locally defined $e-$folding time varies inversely with α_0, as one might naively expect. For ease of viewing we include a dashed line showing $t_{\rm e-fold} = 0$ in the second panel.

Figure 6. The effect of varying the primary mass M_1. The input parameters are the same as before (i.e., $n = 1.5$, $\alpha_0 = 10^{1.7}$, and $N = 1000$), and the small numbers beside each curve indicate M_1 in units of $1M_\odot$. The $e-$folding time is directly proportional to the

central mass. For ease of viewing we include a dashed line showing $t_{\rm e-fold} = 0$ in the second panel.

Figure 7. The effect of varying the orbital period of the binary, keeping other parameters fixed. The small numbers beside each curve indicate the limiting outer disk radius $r_{\rm outer}/10^{11}$ cm, taken to be ~ 0.7 of the Roche radius of the primary.

Figure 8. The variation of the width of the cooling front with radius as the front progresses inward. As earlier, we show moving 50 day averages. This run is for our "standard model" for exponential decay: $n = 1.5$, $\log \alpha_0 = 1.7$, and $M_1 = 10 M_\odot$. The cooling front begins at the right hand side of the graph near $\log r({\rm cm}) = 11$ and moves to the left as the front progresses to smaller radii. The two dashed curves show $\sqrt{h/r}$ and h/r, both evaluated at the outermost "hot" grid point $i_{\rm hot}$. The solid curve gives the front width $w \equiv r(i_{\rm cold}) - r(i_{\rm hot})$, expressed in units of radius. In general, the total width of the front exceeds by some nominal factor the region of greatest variation (Osaki 1989), therefore w/r lies a little above $\sqrt{h/r}$. The dotted curve shows the number of grid points lying inside the cooling front N_F. As N_F drops below unity, we artificially constrain w to equal the grid spacing Δr, and since $\Delta r \propto \sqrt{r}$ in our model, $w/r \rightarrow \propto r^{-1/2}$. Thus w is spuriously dominated by the grid spacing for $\log r({\rm cm}) < 9$.

Figure 9. The variation of the local flow parameters $v_r(r)$ and $\dot{M}(r)$ for the standard model. The dashed lines indicate initial conditions, and the dotted lines show conditions associated with $\Sigma_{\rm max}$ and $\Sigma_{\rm min}$. Each curve is separated by 100 days of evolution. The amplitudes of the local flow speed and the local mass flux decrease with time. For the inner disk radii v_r and $\dot{M}(r)$ are negative, while for the outer radii they are positive. At a given time step roughly the outer half of the hot disk is flowing outward, and roughly the inner half is flowing inward. For the outflow $\dot{M}(r) \propto r^3$, and for the inflow $\dot{M}(r)$ approaches a constant.

Table 1

Effect of Varying $r_{\rm inner}$

r_1(cm)	N^b	$t_{\rm rec}$	$t_{\rm r,3}$	$t_{\rm r,2}$	$t_{\rm r,e}$	$t_{\rm d,e}$	$t_{\rm p}$	$\log \dot{M}_{\rm peak}$
(cm)[a]		(yr)[c]	(days)[d]	(days)[e]	(days)[f]	(days)[g]	(days)[h]	(g s^{-1})[i]
10^9	103	70.8	46	42	29	150	339	18.99
$10^{8.5}$	107	70.5	48	44	30	161	360	18.96
10^8	110	70.3	50	46	30	168	374	18.94
10^9	160	72.7	45	42	29	150	337	19.00
$10^{8.5}$	166	72.4	46	43	29	160	357	18.97
10^8	170	72.2	47	44	30	167	369	18.96
$10^{7.5}$	172	72.0	48	45	31	170	376	18.95

[a] Inner disk radius.

[b] Number of radial grid points.

[c] Recurrence time between successive outbursts.

[d] Rise time for $\dot{M}_{\rm inner}$ to change by 10^3, measured from the time of maximum $\dot{M}_{\rm inner}$.

[e] Rise time for $\dot{M}_{\rm inner}$ to change by 10^2, measured from the time of maximum $\dot{M}_{\rm inner}$.

[f] Rise time for $\dot{M}_{\rm inner}$ to change by e, measured from the time of maximum $\dot{M}_{\rm inner}$.

[g] Decay time for $\dot{M}_{\rm inner}$ to change by e, measured from the time of maximum $\dot{M}_{\rm inner}$.

[h] Time spent on the "plateau" of the outburst.

[i] The maximum value of $\dot{M}_{\rm inner}$.

Table 2

Dependence of Outburst Properties on $\dot{M}_T$

$\dot{M}_T$	N^b	$t_{\rm rec}$	$t_{\rm r,3}$	$t_{\rm r,2}$	$t_{\rm r,e}$	$t_{\rm d,e}$	$t_{\rm p}$	$\log \dot{M}_{\rm peak}$
$(M_\odot\ {\rm yr}^{-1})^a$		(yr)^c	(days)^d	(days)^e	(days)^f	(days)^g	(days)^h	(g s^{-1})^i
0.25×10^{-9}	170	260.5	47	44	30	170	347	18.91
0.5×10^{-9}	170	137.1	48	45	30	169	358	18.93
1×10^{-9}	170	72.2	47	44	30	167	369	18.96
2×10^{-9}	170	38.3	47	43	30	166	388	18.98
4×10^{-9}	170	20.5	46	41	29	166	425	19.00

[a] Mass transfer rate from the secondary star.

[b] Number of radial grid points.

[c] Recurrence time between successive outbursts.

[d] Rise time for $\dot{M}_{\rm inner}$ to change by 10^3, measured from the time of maximum $\dot{M}_{\rm inner}$.

[e] Rise time for $\dot{M}_{\rm inner}$ to change by 10^2, measured from the time of maximum $\dot{M}_{\rm inner}$.

[f] Rise time for $\dot{M}_{\rm inner}$ to change by e, measured from the time of maximum $\dot{M}_{\rm inner}$.

[g] Decay time for $\dot{M}_{\rm inner}$ to change by e, measured from the time of maximum $\dot{M}_{\rm inner}$.

[h] Time spent on the "plateau" of the outburst.

[i] The maximum value of $\dot{M}_{\rm inner}$.

Table 3

Effect of Varying $\alpha_{\rm cold}$ while Keeping $\alpha_{\rm hot}$ Constant

$\alpha^a_{\rm cold}$	N^b	$t_{\rm rec}$	$t_{\rm r,3}$	$t_{\rm r,2}$	$t_{\rm r,e}$	$t_{\rm d,e}$	$t_{\rm p}$	$\log \dot{M}_{\rm peak}$
		(yr)^c	(days)^d	(days)^e	(days)^f	(days)^g	(days)^h	(g s^{-1})^i
0.005	170	145.2	38	35	25	128	465	19.32
0.0075	170	97.4	43	40	27	150	412	19.11
0.01	170	72.2	47	44	30	167	369	18.96

[a] Viscosity parameter along lower branch of $S-$curve.

[b] Number of radial grid points.

[c] Recurrence time between successive outbursts.

[d] Rise time for $\dot{M}_{\rm inner}$ to change by 10^3, measured from the time of maximum $\dot{M}_{\rm inner}$.

[e] Rise time for $\dot{M}_{\rm inner}$ to change by 10^2, measured from the time of maximum $\dot{M}_{\rm inner}$.

[f] Rise time for $\dot{M}_{\rm inner}$ to change by e, measured from the time of maximum $\dot{M}_{\rm inner}$.

[g] Decay time for $\dot{M}_{\rm inner}$ to change by e, measured from the time of maximum $\dot{M}_{\rm inner}$.

[h] Time spent on the "plateau" of the outburst.

[i] The maximum value of $\dot{M}_{\rm inner}$.

Table 4

Effect of Varying Primary Mass M_1

M_1	N^b	t_{rec}	$t_{r,3}$	$t_{r,2}$	$t_{r,e}$	$t_{d,e}$	t_p	$\log \dot{M}_{peak}$
$(M_\odot)^a$		(yr)^c	(days)^d	(days)^e	(days)^f	(days)^g	(days)^h	(g s^{-1})^i
5.0	170	88.9	38	35	24	119	256	19.19
7.5	170	78.7	42	39	27	144	317	19.05
10.0	170	72.2	47	44	30	167	369	18.96
15.0	170	64.0	57	53	37	203	459	18.82
20.0	170	59.5	63	59	40	236	538	18.72

[a] Mass of the accreting black hole.

[b] Number of radial grid points.

[c] Recurrence time between successive outbursts.

[d] Rise time for $\dot{M}_{inner}$ to change by 10^3, measured from the time of maximum $\dot{M}_{inner}$.

[e] Rise time for $\dot{M}_{inner}$ to change by 10^2, measured from the time of maximum $\dot{M}_{inner}$.

[f] Rise time for $\dot{M}_{inner}$ to change by e, measured from the time of maximum $\dot{M}_{inner}$.

[g] Decay time for $\dot{M}_{inner}$ to change by e, measured from the time of maximum $\dot{M}_{inner}$.

[h] Time spent on the "plateau" of the outburst.

[i] The maximum value of $\dot{M}_{inner}$.

Table 5

Effect of Varying $r_{\rm outer}$

r_2	N^b	$t_{\rm rec}$	$t_{\rm r,3}$	$t_{\rm r,2}$	$t_{\rm r,e}$	$t_{\rm d,e}$	$t_{\rm p}$	$\log \dot{M}_{\rm peak}$
$(10^{11}$ cm$)^a$		(yr)^c	(days)^d	(days)^e	(days)^f	(days)^g	(days)^h	(g s^{-1})^i
0.75	170	10.3	32	28	19	119	297	18.24
1.00	170	23.1	36	33	23	136	314	18.54
1.25	170	42.8	43	39	27	152	342	18.77
1.50	170	72.2	47	44	30	167	369	18.96
1.75	170	112.6	53	49	34	180	395	19.11
2.00	170	165.7	56	52	34	196	425	19.25

[a] Outer disk radius.

[b] Number of radial grid points.

[c] Recurrence time between successive outbursts.

[d] Rise time for $\dot{M}_{\rm inner}$ to change by 10^3, measured from the time of maximum $\dot{M}_{\rm inner}$.

[e] Rise time for $\dot{M}_{\rm inner}$ to change by 10^2, measured from the time of maximum $\dot{M}_{\rm inner}$.

[f] Rise time for $\dot{M}_{\rm inner}$ to change by e, measured from the time of maximum $\dot{M}_{\rm inner}$.

[g] Decay time for $\dot{M}_{\rm inner}$ to change by e, measured from the time of maximum $\dot{M}_{\rm inner}$.

[h] Time spent on the "plateau" of the outburst.

[i] The maximum value of $\dot{M}_{\rm inner}$.

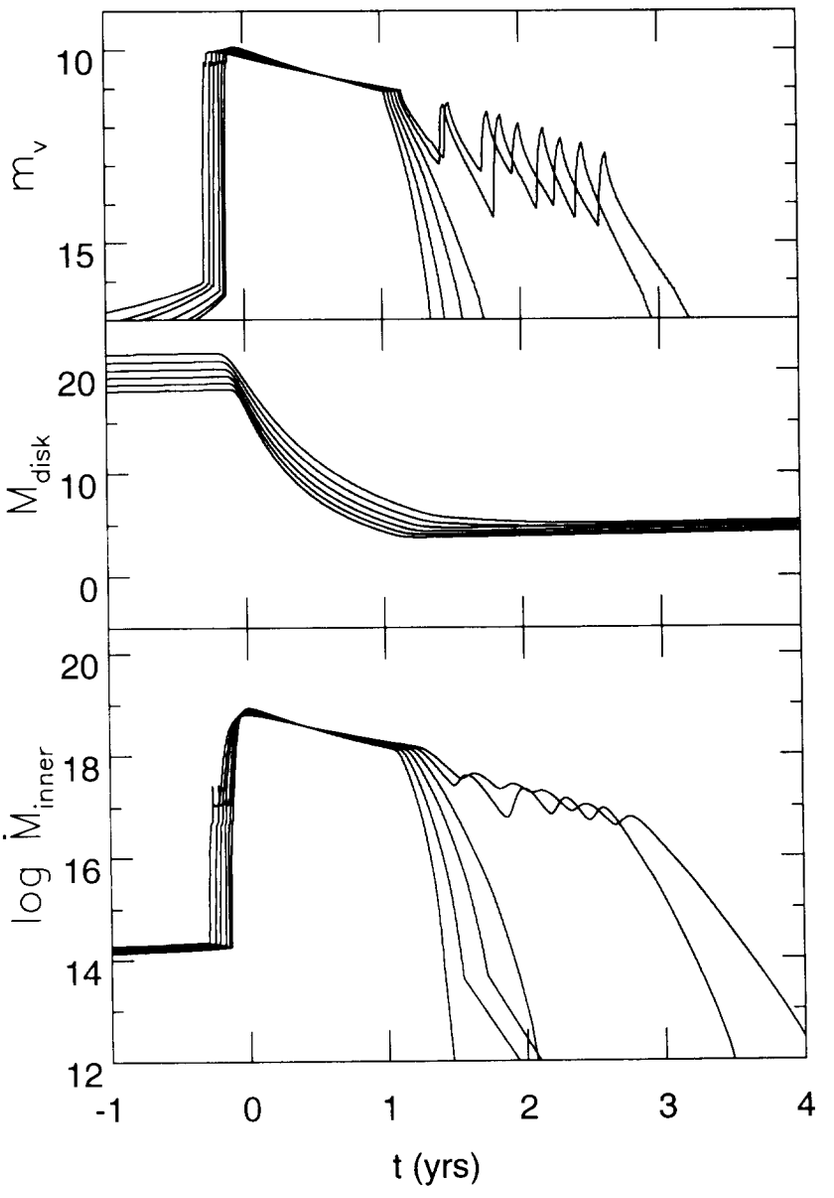

FIGURE 1

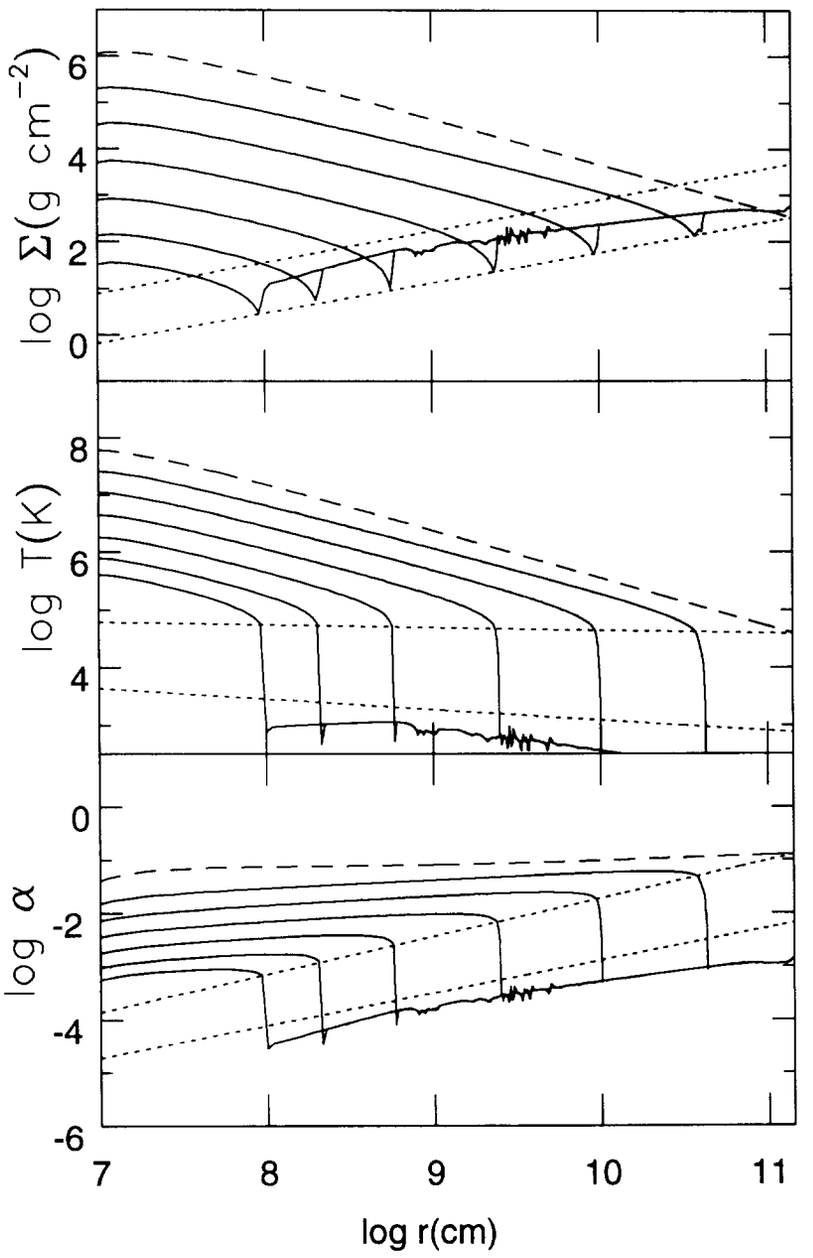

FIGURE 2

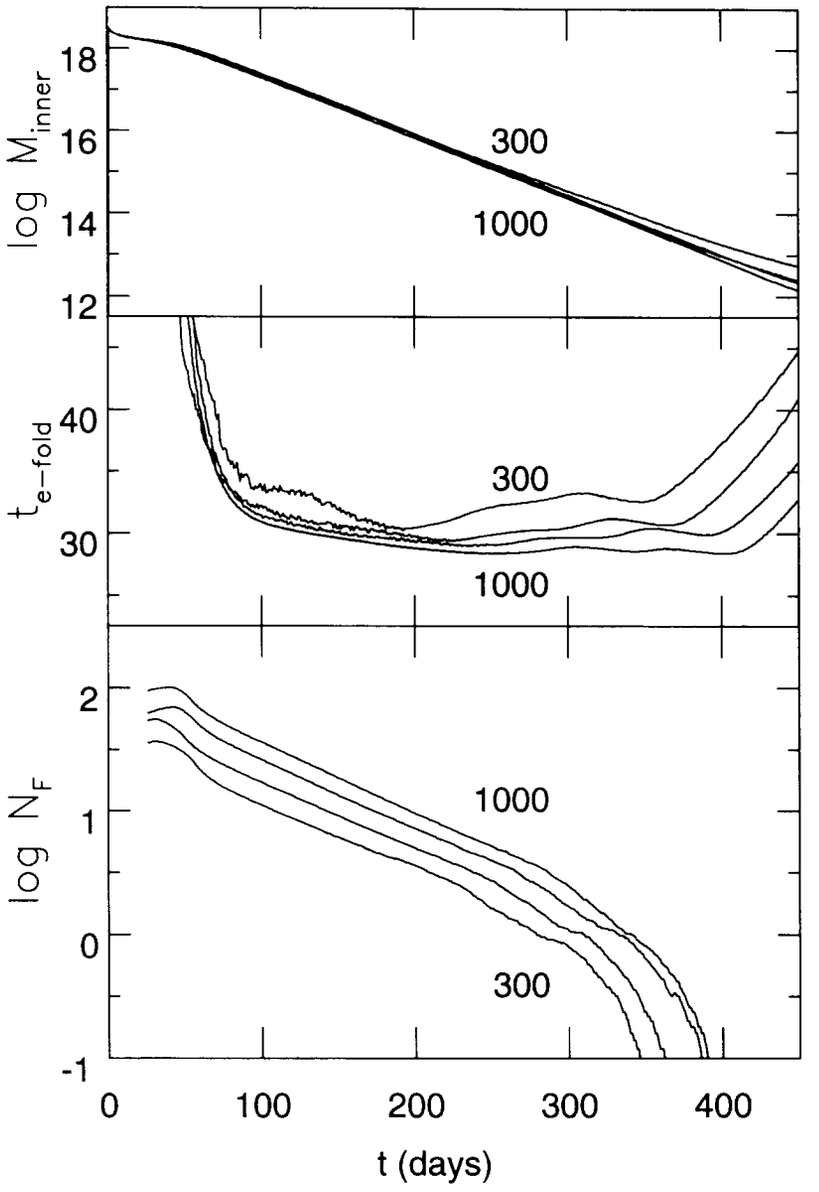
log $\dot{M}_{inner}$
18
16
14
12
300
1000
t_{e-fold}
40
30
300
1000
log N_F
2
1
0
-1
1000
300
0
100
200
300
400
t (days)

FIGURE 3

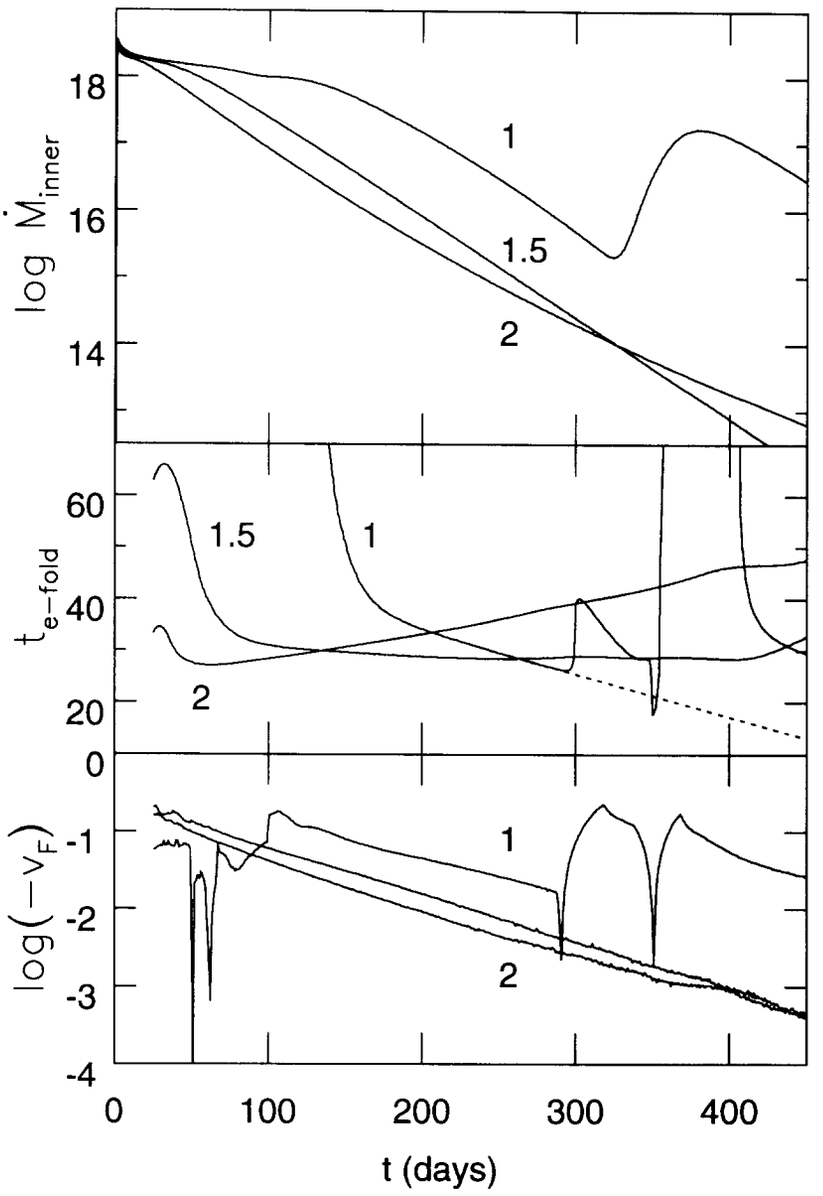
log $\dot{M}_{inner}$
18
16
14
1
1.5
2
t_{e-fold}
60
40
20
0
1.5
1
2
log$(-v_F)$
-1
-2
-3
-4
1
2
0
100
200
300
400
t (days)

FIGURE 4

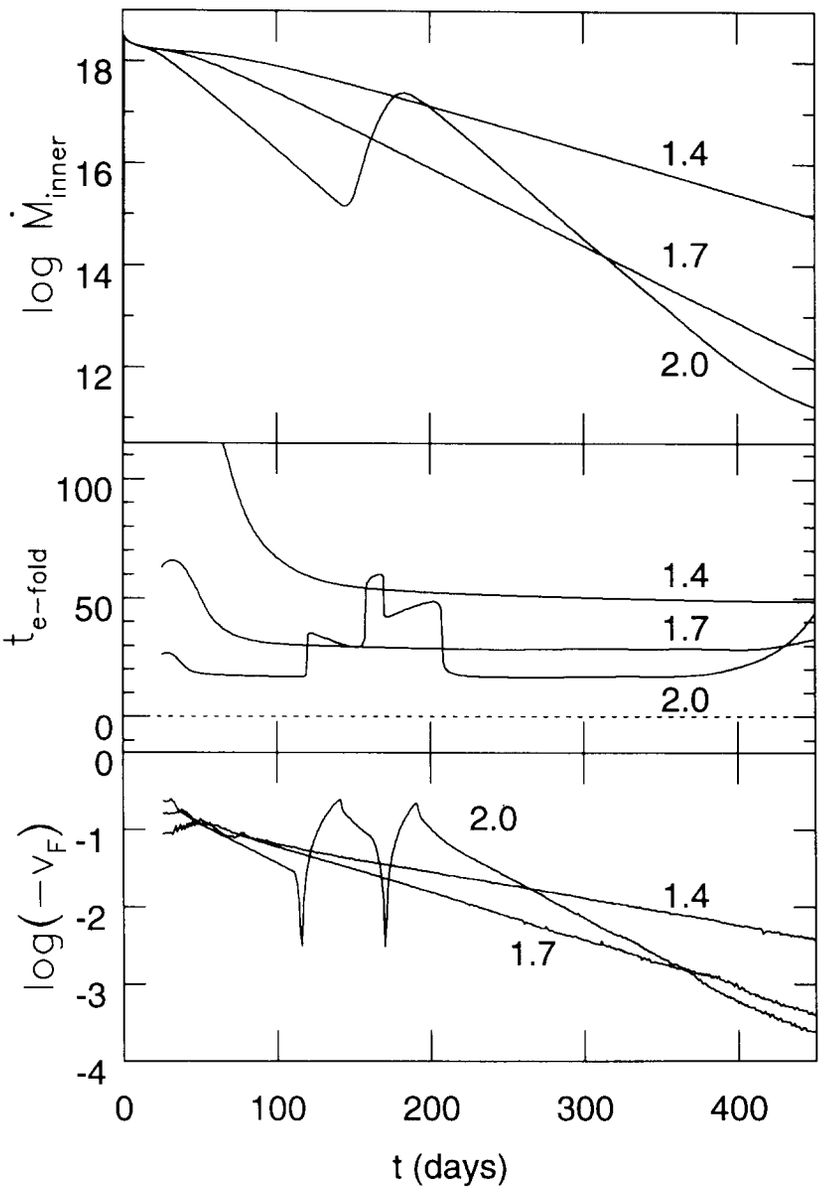
log $\dot{M}_{inner}$
18
16
14
12
1.4
1.7
2.0
t_{e-fold}
100
50
0
1.4
1.7
2.0
0
log$(-v_F)$
-1
-2
-3
-4
2.0
1.4
1.7
0
100
200
300
400
t (days)

FIGURE 5

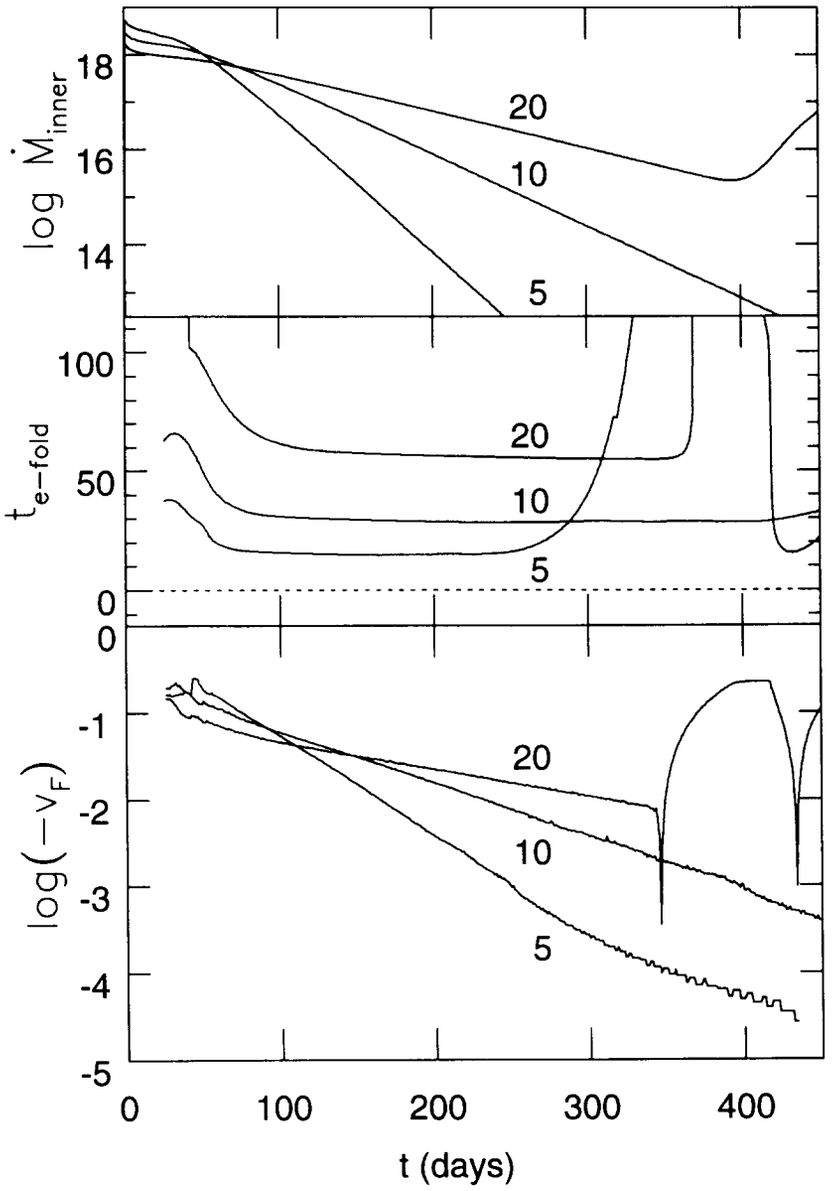
log $\dot{M}_{inner}$
18
16
14
20
10
5
t_{e-fold}
100
50
0
20
10
5
0
log$(-v_F)$
-1
-2
-3
-4
-5
20
10
5
0
100
200
300
400
t (days)

FIGURE 6

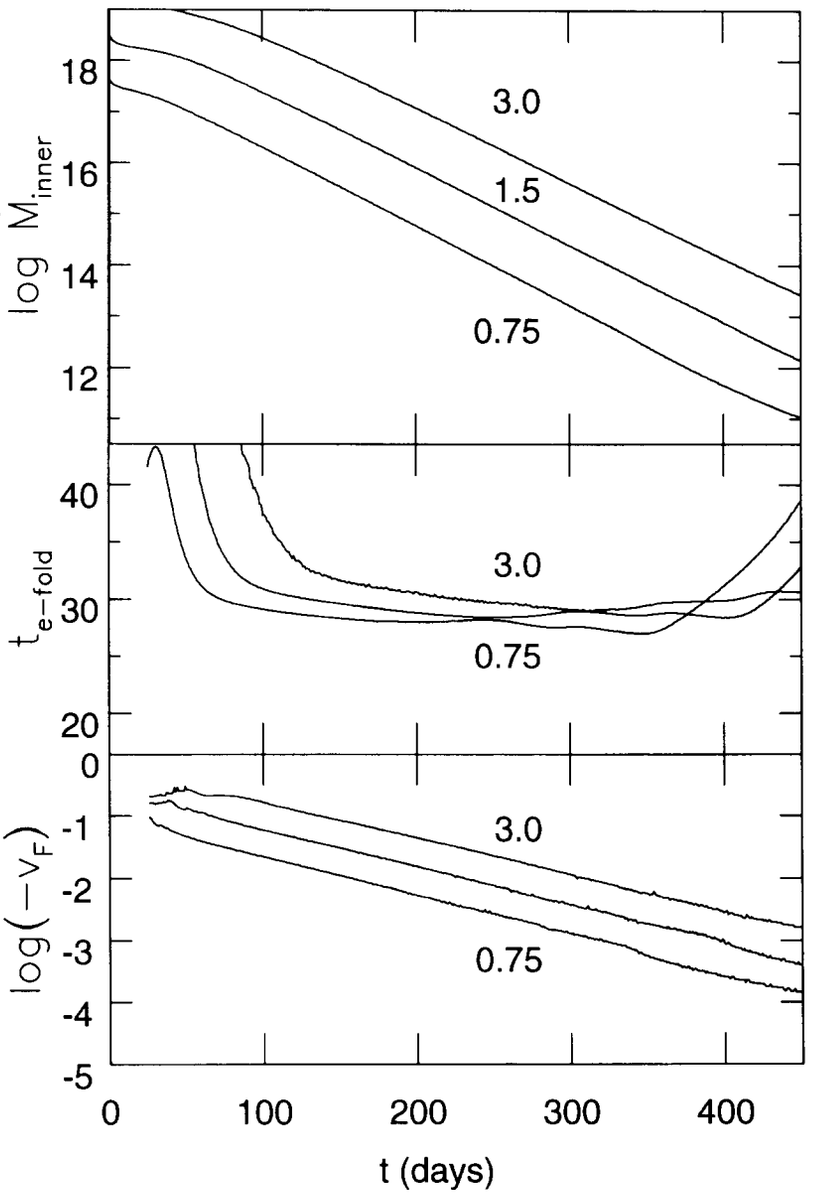
log $\dot{M}_{inner}$
18
16
14
12
3.0
1.5
0.75
t_{e-fold}
40
30
20
3.0
0.75
log$(-v_F)$
0
-1
-2
-3
-4
-5
3.0
0.75
0
100
200
300
400
t (days)

FIGURE 7

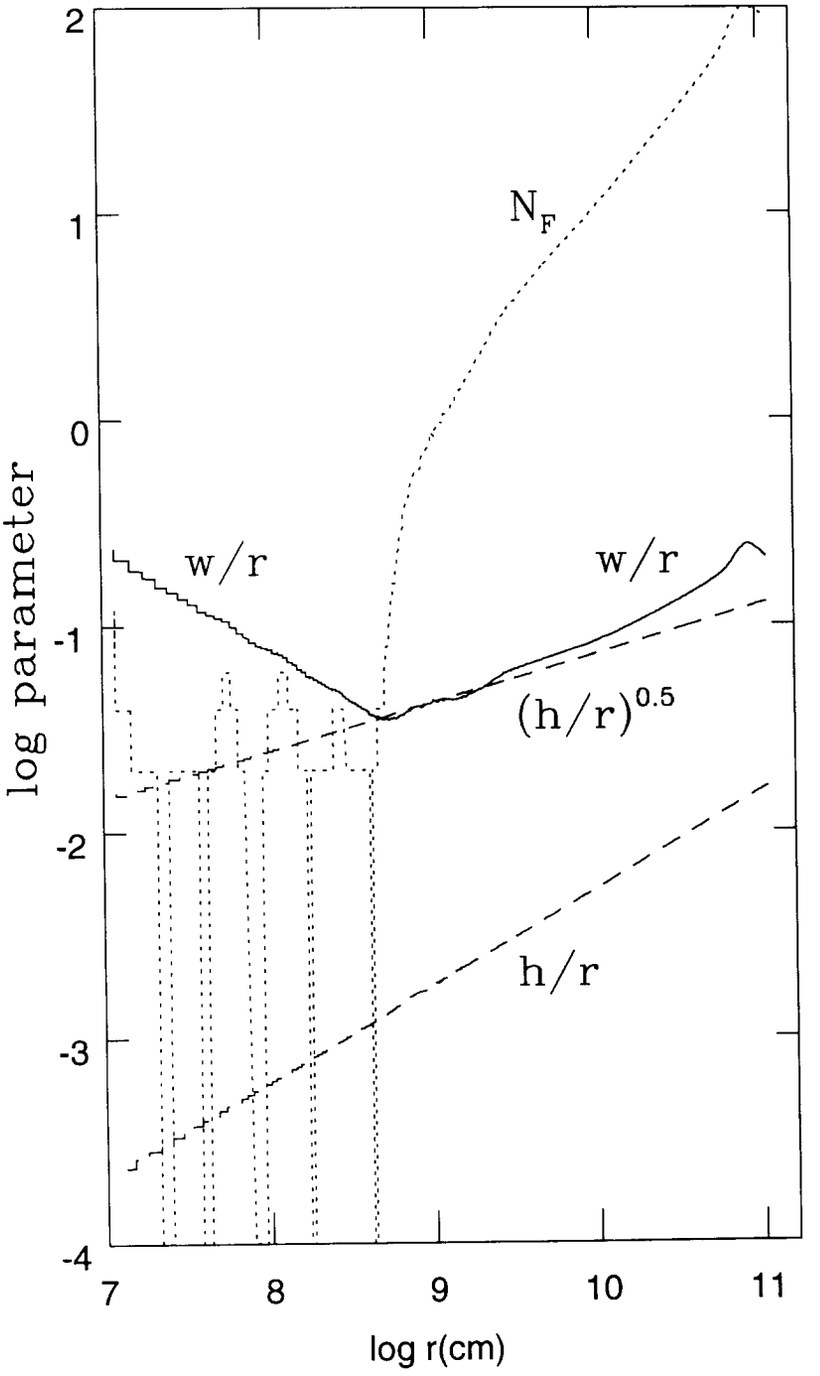

FIGURE 8

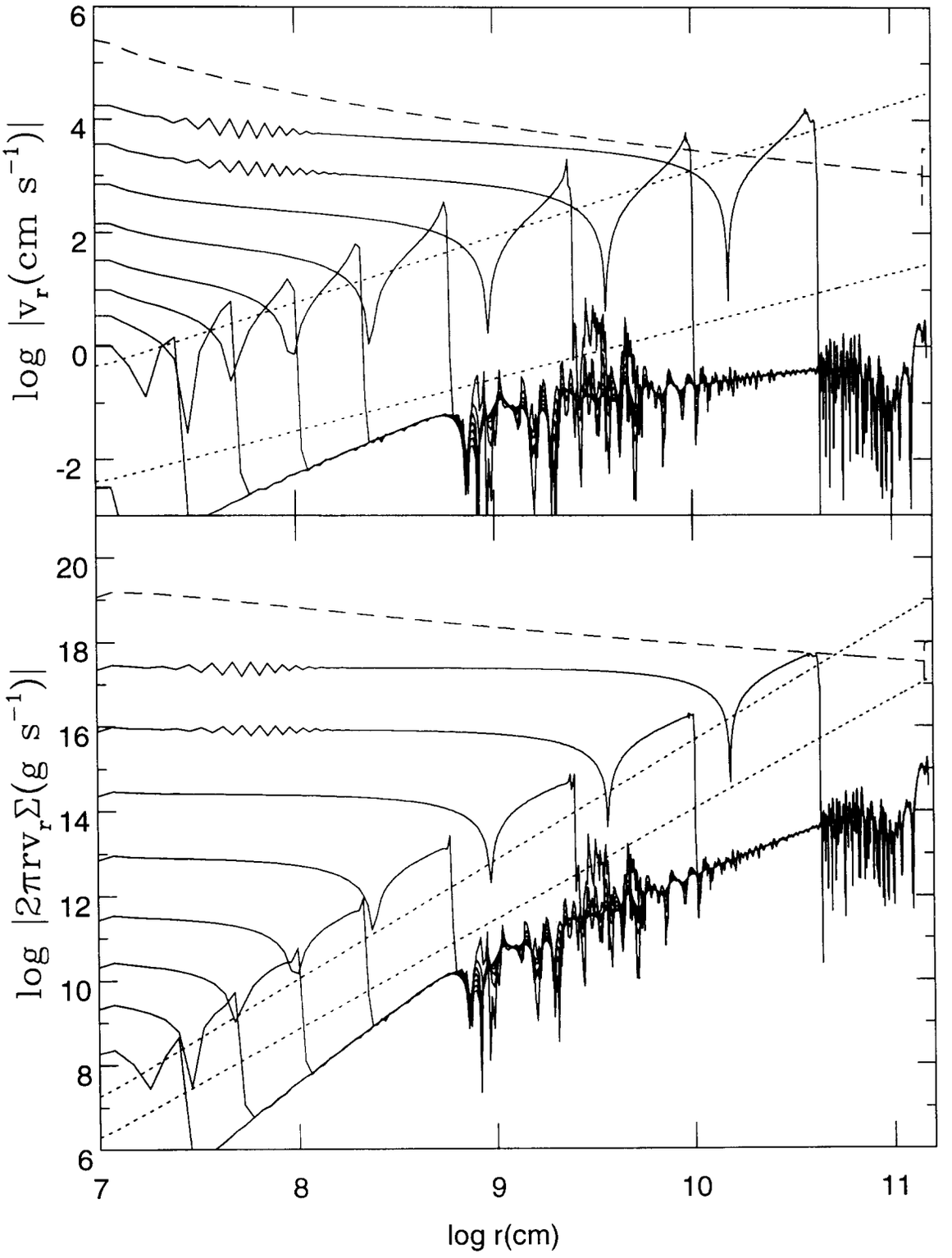
6
4
2
0
-2
log |v_r(cm s^-1)|
20
18
16
14
12
10
8
6
log |2πrv_rΣ(g s^-1)|
7
8
9
10
11
log r(cm)

FIGURE 9